546.57'15:541.183.24:547

MEDEDELINGEN VAN DE LANDBOUWHOGESCHOOL
WAGENINGEN • NEDERLAND • 65-4 (1965)

THE ELECTRICAL DOUBLE LAYER ON SILVER IODIDE IN THE PRESENCE OF ORGANIC MOLECULES

B. H. BIJSTERBOSCH
Laboratory for Physical and Colloid Chemistry, Agricultural University, Wageningen, The Netherlands

(Received 15-I-1965)

H. VEENMAN & ZONEN N.V. – WAGENINGEN – 1965

Mededelingen Landbouwhogeschool Wageningen
65-4 (1965)
(Communications of the Agricultural University)
is also published as a thesis.

CONTENTS

CHAPTER 1

INTRODUCTION

1.1. On the electrical double layer

During the last few decades much attention has been paid to the electrical double layer at charged interfaces. The behaviour of this double layer was studied not only because it is important in itself, but also because it plays a dominant rôle in colloid stability (Derjaguin and Landau, 1941; Verwey and Overbeek, 1948), soil science (van Olphen, 1963), and the kinetics of electrode reactions (see e.g. Frumkin, 1961; Saraby – Reintjes, 1963). Excellent work in this field has been done (reviewed by Haydon, 1964) with the mercury-solution interface as carrier of the charge. This system has several attractive properties:

1. mercury is obtained rather easily in a pure state, and the dropping mercury electrode has a well-defined geometry,
2. being a liquid the surface of mercury can be renewed frequently, so that contamination can be avoided,
3. the mercury-electrode is ideally polarizable over a rather large range of charge and potential, which means that the magnitude of these parameters can be fixed without changing the composition of the solution because there is no flow of charge through the interface,
4. the mercury-solution double layer can be investigated by three independent methods: a. direct determination of the surface charge, b. determination of electro-capillary curves and c. direct measurement of differential capacity. After appropriate calculations these methods give the same information (Grahame, 1947).

One of the drawbacks of the mercury system is its 'missing link' in connection with colloid stability because it is difficult to prepare suitable mercury sols. However, some kind of 'missing link' with respect to this, has been provided very recently by Watanabe and Gotoh (1963).

In order to test the general validity of double layer characteristics found on mercury, and also because of their intrinsic importance, several double layer experiments have also been performed with other systems. Prominent among them is the system AgI-aqueous solution (Verwey and Kruyt, 1933; de Bruyn, 1942; Mackor, 1951; van Laar, 1952; Lijklema, 1957; Lyklema and Overbeek, 1961 b) which is closely related to the AgI sol of which also many properties, such as flocculation values and electrokinetic parameters, are known (Klompé, 1941; Kruyt and Klompé, 1942; Overbeek, 1952; Gutoff, Roth and Steigmann, 1963).

As compared to the mercury system, the AgI system has some definite disadvantages with which we have to cope, viz.:

1. a much smaller range of charge and potential can be covered, which restricts the use of certain extrapolation procedures. In connection with this we note that the AgI-solution interface is reversible: charge and potential are determin-

ed by the adsorption of potential determining ions (Ag^+ and I^-), i.e. by transfer of charge across the interface. This makes the origin of charge and potential different in principle from the ideally polarizable mercury-solution interface,

2. a part of the interfacial potential drop is located in the solid phase, because AgI behaves like a semiconductor in contradistinction to the conductor mercury,
3. there is a greater possibility of contamination, because the surface cannot be renewed,
4. uncertainty exists about the value of the specific surface area, see LIJKLEMA (1957),
5. a long time is needed for every experiment, because establishment of adsorption equilibrium is often slow.

Other sol-precipitate combinations have been considered, but appear to be less attractive for several reasons, such as lack of reproducibility or a smaller accessible potential range. As examples we mention the systems Ag_2S-solution (IWASAKI and DE BRUYN, 1958), Fe_2O_3(α-hematite)-solution (PARKS and DE BRUYN, 1962) and AgBr-solution (BASINSKI, 1941; HERZ and HELLING, 1962).

1.2. THE ELECTRICAL DOUBLE LAYER ON AgI

Recent studies on the double layer on AgI are those of LIJKLEMA (1957) and AGAR (1961). AGAR determined the adsorption of bases and their conjugated acids at the AgI-solution interface, while LIJKLEMA investigated the influence of the nature of counter-ions on the differential double layer capacity. LIJKLEMA found by a potentiometric titration procedure that the capacity of the STERN-layer[1] on negatively charged AgI is much more dependent on the nature of the counter-ion than it is on mercury.

When prepared from $AgNO_3$ and excess KI, AgI has a hexagonal structure, in which the spatial arrangement of the ions is almost identical to those of the water molecules in ice (BRYANT, HALLETT and MASON, 1959). Accordingly the adsorbed water layer may be strongly ordered, thereby imparting structural characteristics to the STERN-layer on AgI which are absent on Hg. Along this line LIJKLEMA (1961) explained the experimentally found differences mentioned above. (In connection with this structure formation we mention the use that is often made of AgI as a condensation nucleus in cloud seeding and related experiments [KATZ, 1961]).

In a recent paper of LYKLEMA and OVERBEEK (1961a) it was shown to what extent formation of water structure at the surface would have implications in electrokinetic phenomena.

1.3. OUTLINE OF PRESENT DOUBLE LAYER INVESTIGATIONS ON AgI IN THE PRESENCE OF NEUTRAL ORGANIC MOLECULES

Recent experiments on the Hg-system are focussed to a large extent on double layer properties in the presence of adsorbed neutral organic compounds.

[1] For a detailed discussion on double layer models, the reader is referred to GRAHAME (1947) or to OVERBEEK (1952).

Because adsorption of an organic compound will modify any existing water structure, it was considered worthwhile to investigate the electrical double layer on AgI also under these circumstances. It can thus be established whether the qualitative relationship between both systems, observed so far, is maintained.

Through their influence on the water structure at the interface and the change in viscosity in the bulk solution organic compounds will affect the location of the slipping plane in electrokinetics. Therefore, electrokinetic measurements with AgI in the presence of organic compounds were also considered to be useful.

In the course of the investigations it turned out that the direct double layer experiments were more reliable and gave more conclusive results than measurements of electrokinetic phenomena, and for this reason the greater part of the following discussion is devoted to the properties of the electrical double layer on AgI in the presence of organic compounds.

CHAPTER 2

DOUBLE LAYER INVESTIGATIONS ON SILVER IODIDE. EXPERIMENTAL

2.1. Determination of surface charge as a function of cell potential

2.1.1. *Principle*

The starting point of the double layer investigations on AgI is the determination of the surface charge as a function of surface potential. As has been described earlier by de Bruyn (1942), van Laar (1952), Mackor (1951), Lijklema (1957) and Lyklema and Overbeek (1961 b), this determination is performed by potentiometric titration of a AgI suspension with potential determining ions. For this titration a solution containing indifferent electrolyte and potential determining ions, both of known concentration, and a known amount of AgI precipitate are brought together in a glass beaker. In the solution are placed a Ag/AgI electrode and a reference electrode.

The EMF of this cell minus the cell-EMF corresponding to the zero point of charge equals the surface potential ψ_0 (Lijklema, 1957; Lyklema and Overbeek 1961 b). After each addition of potential determining ions the surface charge, σ, is found by material balance, using the Nernst equation to calculate the equilibrium concentrations of the potential determining ions Ag^+ and I^-.

2.1.2. *Experimental set-up*

The experimental set-up for the titrations was essentially the same as those described by van Laar (1952) and Lijklema (1957), but some improvements were introduced which led to better reproducibility and accuracy, which was necessary for interpretation of the titrations in the presence of organic compounds. Our arrangement will be given therefore in detail.

Potentiometer. EMF's were measured with a Philips pH-meter, type GM 4491, with an input-impedance higher than 10^4 $M\Omega$, and a precision better than 0.5 mV.

AgI *electrodes* were made by coating a Pt wire with silver by electrolysis in a $KAg(CN)_2$ solution for two hours at 2.5 mA/cm^2, according to Brown (1934) as modified by Agar (1961). (Pt wire: diameter 0.5 mm; sealed in Pyrexglass). The electrodes were rinsed several times with double distilled water and iodized in a 2% KI solution for half an hour at a current density of 2.5 mA/cm^2, followed again by careful rinsing with water. The average reading of at least six electrodes was used in every titration; individual readings differed less than 2 mV at the smallest and less than 0.5 mV at the highest concentrations of potential determining ions.

As *reference electrode* we used a 0.1 *N* KCl calomel-electrode. The electrode potential of this calomel-electrode has a temperature fluctuation of only 0.09

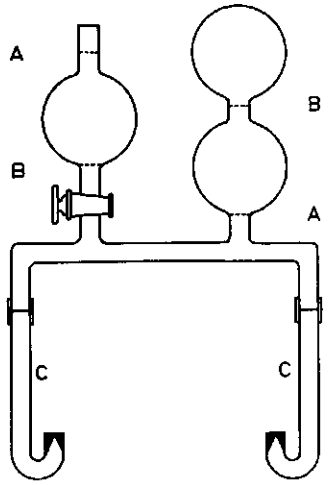

FIGURE 2–1. TWO VAN LAAR capillaries, C, attached to the apparatus for application of extra pressure. A: levels of solution at atmospheric pressure; B: levels of solution at about 1 atmosphere extra pressure

mV/degree^{-1} as compared to 0.66 mV/degree^{-1} for the saturated KCl calomel-electrode (IVES and JANZ, 1961).

Calomel-electrode and solution were linked through two VAN LAAR salt bridges (1955) filled with the 1.75 *N* KNO_3 + 0.25 *N* $NaNO_3$ mixture recommended by VAN LAAR. This mixture suppresses the liquid junction potential as efficiently as KCl, and has the advantage that it does not contaminate the solution with chloride.

The Cl^- ions of a KCl-filled salt bridge used in an earlier stage of the experiments, may have caused the erroneous results we found at that time. In making the capillaries extreme care was taken that the electrical resistance did not amount to more than about 1.5 *M*Ω, in order to avoid misleading potential measurements. The extra pressure under which the solution has to be placed in the salt bridges was applied with an arrangement suggested by Dr. R. S. HANSEN (Fig. 2–1).

The *titration vessel* was a 600 ml Pyrex beaker, with a Perspex cover in which openings for the electrodes, the salt bridge, a N_2 inlet and the stirrer. The beaker was externally coated with dimethyldichlorsilane to make it more hydrophobic, in order to suppress current leakages. All other glassware used was made of Pyrex. It was cleaned with hot chromic acid and cold diluted nitric acid, and steamed before use.

Thermostat. Water of 20 ± 0.1 °C was circulated through a Perspex box surrounding the beaker. This temperature is close to the average room temperature in LYKLEMA's experiments but five degrees lower than in those of VAN LAAR. 20 °C is preferable because evaporation of solvent from the beaker, followed by condensation on the Perspex cover and falling back of droplets with possible impurities is smaller than at 25 °C.

2.1.3. *Materials*

All water used was twice distilled from a normal laboratory still and then once from an all-tin kettle with a silver cooler. Before use it was percolated through a column of AgI precipitate to remove adsorbing impurities, if any.

$AgNO_3$ and KI were supplied by Union Chimique Belge S.A. with a high degree of purity (better than 99.9 %). They were not recrystallized.

AgI precipitates were made by addition of 0.1 *N* $AgNO_3$ solution to 2 l of a well stirred 0.1 *N* KI solution through which N_2, purified by BTS catalyst from Badische Anilin und Soda Fabrik, was bubbled. The rate of addition was about 0.1 l/hr during the first quarter of an hour, but from then on increased to about 1 l/hr. Addition was stopped when the zero point of charge, *z.p.c.*, was reached; stirring was continued then for about an hour to reach equilibrium. The precipitate was washed several times with conductivity water and aged for three days at 80 °C, in a solution of initially pI = 4 in a Pyrex vessel. Ageing was necessary in order to have a constant specific surface area during the titrations (LIJKLEMA, 1957).

It is not critical to add $AgNO_3$ to KI, for addition of KI to $AgNO_3$ gave a precipitate with indistinguishable adsorption properties, provided the rest of the procedure was the same.

KNO_3 was Analar grade (B.D.H.); it was recrystallized twice before use.

Urea (Analar B.D.H.) and thiourea (B.D.H.) were used without further purification.

Alcohols (B.D.H.) were carefully distilled before use. Only the middle fractions (boiling point range less than 0.3 °C) were employed.

2.1.4. *Electrochemistry of the cell*

The cell described has several phase boundaries but as the diffusion potential at the boundary solution-VAN LAAR capillary is presumed to be constant, only the potential at the interface AgI electrode-solution changes by changing the composition of the solution.

According to NERNST the relation between the potential E_e of the AgI electrode and the activity, a, of potential determining ions in solution is given by

$$E_e = E_{0,Ag} + (RT/F) \ln a_{Ag^+} = E_{0,I} - (RT/F) \ln a_{I^-} \qquad (2\text{–}1)$$

In this equation R, T and F have their usual meaning, while $E_{0,Ag}$ and $E_{0,I}$ are constants, numerically equal to the electrode potential, when $\ln a_{Ag^+}$ and $\ln a_{I^-}$ are zero respectively. Eq. (2–1) can also be written as

$$E_e = E_{0,Ag} + (RT/F) \ln f_{Ag^+} c_{Ag^+} = E_{0,I} - (RT/F) \ln f_{I^-} c_{I^-} \qquad (2\text{–}2)$$

where c = concentration and f_{Ag^+} and f_{I^-} are activity coefficients.

For 20 °C eq. (2–2) can be modified further to

$$E_e = E_{0,Ag}' - 58 \text{ pAg} = E_{0,I}' + 58 \text{ pI} \qquad (2\text{–}3)$$

where $E_0' = E_0 + (RT/F) \ln f$; pAg and pI stand for the negative BRIGGSIAN logarithms of the Ag^+ and I^- concentration, and 58 is the value of 2.3 RT/F at 20°C.

E_0' is a constant as long as the ionic strength of the solution is constant, but changes when the ionic strength is altered. In none of our experiments was the constant concentration of indifferent electrolyte (*IEC*) lower than 10^{-3} N, and as the maximum concentration of potential determining ions was 10^{-4} N, eq. (2–3) may be applied therefore with constant E_0'. When all the other (constant) potential junctions are taken together with E_0' to give the constant E_0'', the cell-EMF, E, can finally be written as

$$E = E_{0,Ag}'' - 58 \text{ pAg} = E_{0,I}'' + 58 \text{ pI} \qquad (2\text{–}4)$$

Values of $E_{0,Ag}''$ and $E_{0,I}''$ can be determined by measuring the cell-EMF when the solution contains the desired *IEC* and a known concentration of Ag^+ or I^- ions. The AgI suspension is added in order to provide a large adsorbing surface area; it is assumed that at equilibrium ψ_0 (electrode) = ψ_0 (particles).

2.1.5. *Standardization*

Values of E_0'' were determined with solutions of known composition (*IEC* $\gg$ Ag^+ and I^- concentrations). In the beginning we only used solutions of pAg(pI) 4 and 5. MIRNIK and DESPOTOVIC (1960), however, claimed to have established that the NERNST equation in the AgI case is invalid at potential determining ion concentrations of 10^{-6} N or less, (experimentally observed deviations of a few hundred millivolts were quoted) which would invalidate our standardization procedure. In order to check the MIRNIK – DESPOTOVIC statement we performed experiments at Ag^+ and I^- concentrations of 10^{-7} N. These very low concentrations were made by dilution of standard solutions of 10^{-3} N in a graduated flask in which a small amount of AgI was present. The cell-EMF due to this solution was measured and then a new solution was made in the same glass-ware and used for another measurement. Following this procedure several times we ascertained that the AgI precipitate and the glass-walls were in equilibrium with solution of the calculated concentration. In fact after about six or seven runs the EMF value became constant. It differed less than 10 mV from the value calculated from the NERNST equation using the E_0'' found at pAg(pI) 4. We believe that this is sufficient indication of the correctness of this equation, and that it also applies at low concentrations.

The addition of an organic compound to the solution at given *IEC* influences the activity coefficient of the ions, and the diffusion potential. These quantities being part of E_0'', it is necessary to redetermine this parameter in the presence of these compounds. This has been done for all compounds investigated and the change in E_0'' was usually not more than a few mV's at the highest concentrations.

2.1.6. *Titration procedure*

The actual experiments usually started at the cell-EMF corresponding with the zero point of charge (VAN LAAR, 1952). After addition of a known volume of a 10^{-2} *N* solution of PD ions and equilibration a new constant value of the cell-EMF, *E*, was reached, the change in *E* giving the change in GALVANI potential difference at the AgI-solution interface. At the same time from *E* the new concentration of PD ions in solution was calculated. From material balance the number of adsorbed PD ions was found; these constitute the surface charge σ. After equilibration the procedure was repeated to give a new combination of σ and *E*, and so on. By plotting the surface charge vs. the cell-EMF, at constant *IEC* an adsorption isotherm was obtained from which the differential capacity could be derived by differentiation.

In chapter 1 it was mentioned already that investigations were carried out in the presence of organic compounds.

The procedure under these circumstances was essentially the same as described above. We always started with the determination of the $\sigma - E$ relation for the base solution. At the maximum negative or positive surface charge a certain amount of organic compound was then added, together with a calculated amount of *IE* in order to keep the ionic strength constant. The solution was then titrated with the standard solution required to change the sign of the surface charge, until the maximum in opposite charge was reached. A new amount of compound, together with *IE*, was added, the titration direction reversed, and so on.

Concentrations of organic compounds were found by determination of the refractive index of the solution with an ABBE refractometer.

The weight of the AgI sample was always measured after a set of adsorption measurements had been completed. The precipitate was washed till electrolyte-free, dried at 110°C and weighed. All experiments were performed with about 50 gram of AgI.

2.1.7. *Accuracy and reproducibility*

Several experimental factors can influence the accuracy and reproducibility of the titrations, most of them being reflected in the value of σ. It is not feasible to discuss them all in detail, but it can be said that e.g. temperature, electrical cell resistance and attainment of the equilibrium cell-EMF were controlled carefully. Changes in the volume of the solution, caused by evaporation, and by addition of standard solutions were accounted for. Standard solutions of potential determining ions were added by means of a pipette, thus introducing smaller errors than with the use of a burette, while contamination of the solution by stopcock grease is avoided.

One way to check the overall reproducibility of the experiments is to compare the σ–*E* relationship for two successive titrations on the same AgI sample, one titration being performed from positive to negative surface charge, the other in the opposite direction. Fig. 2–2 shows that the points lie evidently on one single line, thus showing that the reproducibility is quite satisfactory.

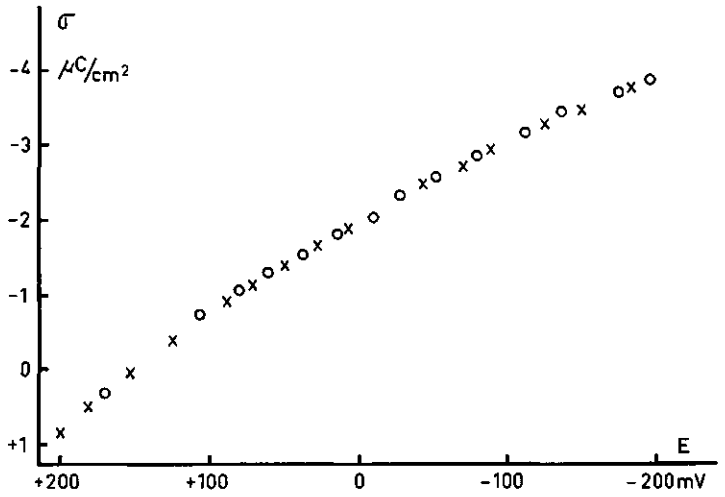

FIGURE 2–2. Surface charge, σ, as a function of cell-EMF, E, in 10^{-1} N KNO_3, as derived from two successive titrations on the same AgI sample. x titration from positive to negative surface charge; 0 titration in the opposite direction

2.2. DETERMINATION OF ZERO POINTS OF CHARGE IN THE PRESENCE OF ALCOHOLS

2.2.1. *Experimental set-up*

Zero points of charge were determined by the streaming potential technique, using the apparatus of fig. 2–3 which is essentially the same as that employed by BUCHANAN and HEYMANN (1948). This apparatus consists of two separate glass tubes (C and D), held together by means of the glass ball joint G. Tube C is connected with two glass bulbs by means of glass joints. Both glass bulbs are provided with a gas inlet (E and F). In tube C a Pt plate, A, containing a large number of holes with a diameter of 0.1 mm, is sealed in. From this plate a Pt wire leads to the closed end of the tube where it protrudes. Another perforated Pt plate, B, attached to tube D via the connecting Pt wire H fits snugly into tube C. The plates A and B serve as electrodes, and as containers for the AgI plug to be investigated.

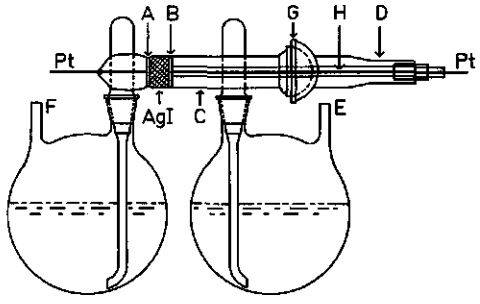

FIGURE 2–3. Apparatus for streaming potential measurements. Explanation in the text.

Streaming potentials arising between the two protruding Pt wires at pressing the liquid through the AgI plug, were measured with a Keithley Electrometer Amplifier type 603.

Pressures were applied at E and F via a device containing an artificial leak. This leak became effective when the manometer, to which it was coupled via a relay, indicated too high a pressure. The principle of this arrangement has been described by OOSTERMAN (1937).

2.2.2. *Experimental procedure*

At the start of each experiment the pAg of the AgI suspension (in 10^{-3} N KNO_3 and a known concentration of organic compound) was determined in the cell described in sections 2.1.4. and 2.1.5. The equilibrium solution was then transferred to the two bulbs of the streaming potential apparatus, and the suspension was compressed to give a tight plug between the electrodes A and B. The whole apparatus was then filled with the solution from the bulbs, pressure was applied and the streaming potential determined.

In order to avoid spurious potentials we adopted the following measuring procedure, recommended by KORPI (1960). The solution was forced through the plug from right to left and the reading of the potentiometer (V_1) recorded. The pressure was then suddenly released and the new potentiometer reading (V_2) recorded. The solution was then forced from left to right at the same pressure P, and the same procedure was applied. The two values of $(V_2 - V_1)$ thus obtained differed 20 % at most; their average value was interpreted as the streaming potential V. When plotted as a function of P, V gave a straight line, as shown in fig. 2–4. It should be noted that this line does not pass through the origin. The intercept of the V-axis is not large however.

Determinations were performed at several values of the pAg, corresponding to both positive and negative surface charge, and the slopes of the $V-P$ relations were plotted as a function of pAg. The intersection with the pAg axis

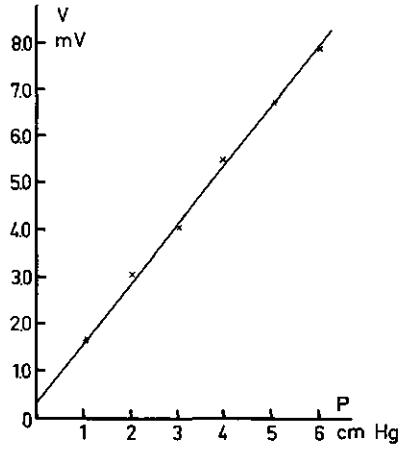

FIGURE 2–4. Streaming potential, V, as a function of applied pressure, P, for a AgI plug in equilibrium with a 10^{-3} N KNO_3 solution (pAg 4.06) containing 0.40 mole/l n-butyl alcohol

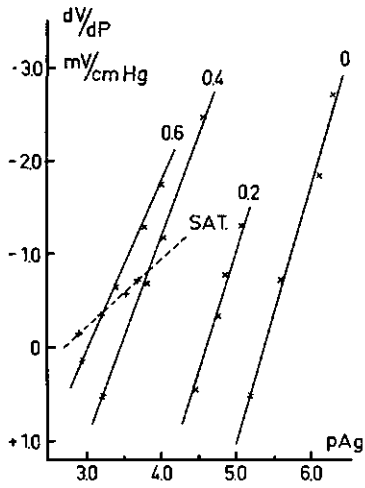

FIGURE 2–5. *dV/dP* (see text) as a function of pAg for various concentrations (mole/l) of n-butyl alcohol in 10^{-3} *N* KNO_3 solution

when $dV/dP = 0$, of the line through these points gave the pAg at the *z.p.c.* at the existing concentration of organic compound; for an example see fig. 2–5. By proceeding in this way for several concentrations c_a of the organic compounds, the shift in the zero point of charge was determined as a function of c_a.

CHAPTER 3

ELECTROKINETIC MEASUREMENTS

3.1. INTRODUCTION

In electrokinetic phenomena one deals with the combination of electrical effects and the tangential movement of two separate phases with respect to each other. In many cases one phase is colloidally dispersed in the other. In the interpretation of these phenomena it is often assumed that the slipping plane, forming the boundary between the two phases, coincides under all circumstances with the separation between STERN and GOUY layer. This implies that ζ, the potential at the slipping plane with respect to the solution at large distance, and ψ_δ, the potential drop in the GOUY-CHAPMAN diffuse double layer, are set equal. No explicit argumentation for this assumption can be given, and although this model can explain several results rather well (OVERBEEK, 1952; SCHENKEL and KITCHENER, 1960; OTTEWILL and RASTOGI, 1960; SRIVASTAVA and HAYDON, 1964), in general it is too simple.

LYKLEMA and OVERBEEK (1961 a) recently published a more fundamental approach to the mechanism that determines the place of the slipping plane with respect to the phase boundary. In their approach, as applied to electrophoresis, they take into account a variable value of the viscosity in the double layer, a parameter assumed to be constant in former derivations of electrokinetic equations. Factors that can possibly influence the viscosity i.e. the electrical field strength in the double layer (viscoelectric effect) and geometrical factors e.g. structural effects on the solvent at the surface of the dispersed particle, are considered. When the geometrical factors preponderate, i.e. at low double layer potential, the slipping plane is situated at a constant distance from the particle surface, and ζ increases with increasing values of ψ_δ. When ψ_δ exceeds a certain value, however, the influence of the field strength on the viscosity increases and finally surpasses the influence of the structural factors and the slipping plane gradually shifts in an outward direction, while becoming a slipping layer rather than a slipping plane. This is reflected by an apparent constancy of the observed electrokinetic quantity with increasing ψ_δ. This last mentioned behaviour will also be observed when structural factors are absent, and can be interpreted as if the slipping plane initially coincides with the separation between STERN and GOUY layer, which is thus only a limiting case in this model.

LYKLEMA and OVERBEEK give some experimental examples in support for their theory, but for a thorough test one should have available large sets of reliable ψ_δ–ζ combinations under several circumstances, in a system in which both viscosity-influencing factors are operative. Such a system is the AgI-solution interface, in which the waterstructure at the interface is the structural factor, while the electrical field strength in the double layer can be made so high that the viscoelectric effect also becomes operative, at least when the visco-

electric constant has the rather large value calculated by LYKLEMA and OVERBEEK.

The adsorption of organic molecules at the interface will destroy the existing structure. Hence, electrokinetic measurements in the presence of adsorbable organic molecules can possibly discriminate between the two viscosity determining mechanisms.

3.2. ELECTROPHORESIS MEASUREMENTS WITH AgI SOLS

Electrophoresis measurements provide the electrophoretic mobility (*E.M.*), the velocity of the dispersed particle per unit field strength. According to the theory of electrophoresis, the most advanced version of which is given by WIERSEMA (1964), several conditions have to be fulfilled in order to make conversion of *E.M.* into ζ-potentials possible. Among these is the prerequisite that the particles should be spherical, and this is certainly not the case with AgI particles, neither when they are made in the way described by TROELSTRA (1941), nor when monodisperse sols are prepared according to the methods of EDWARDS, EVANS and LA MER (1962), or OTTEWILL and WOODBRIDGE (1961). As the theory for polygonal particles is not developed as yet, there is no better method than to use the theory for spherical particles. It should be realized however that in doing so uncertainties are introduced.

Another prerequisite is that the particles are non-conducting. With respect to this point we refer to section 3.3. where it is shown that AgI particles also do not satisfy this condition.

When AgI sols are prepared in the usual way by mixing $AgNO_3$ and KI solutions, followed by electrodialysis and ageing (see TROELSTRA, 1941), the AgI particles have radii between 500 and 1000 Å, as found by electron microscopy. In a 10^{-3} *N* KNO_3 solution this corresponds to $\varkappa a$ values between 5 and 10, where $\varkappa$ is the reciprocal thickness of the diffuse double layer, and a is the radius of the spherical particle. From WIERSEMA's calculations it appears that the effect of relaxation for a sol containing 1 – 1 electrolyte is maximal when the value of $\varkappa a$ is in the neighbourhood of 5, so that our sols require a relatively large relaxation correction.

The *E.M.*'s of sols of $\varkappa a$ about 7 were measured as a function of pAg at 20°C at a solconcentration of 5.10^{-5} mole AgI per liter 10^{-3} *N* KNO_3 solution. The micro-electrophoresis apparatus used, was essentially the same as the one described by MACKOR (1951). Particle velocities were measured at the two depths in the closed cylindrical cell at which the solvent is calculated to be at rest (VAN GILS and KRUYT, 1936). These velocities differed usually not more than 10 %, and their average value was taken as the correct velocity. The field strength causing the AgI particles to move was calculated from the cell dimensions, the current flowing through the cell and the specific conductivity of the sol (HUNTER and ALEXANDER, 1962). Before use the cell was cleaned with chromic acid, leached with borax solution and rinsed with a large amount of water to remove possibly interfering silicate ions (DOUGLAS and BURDEN, 1959).

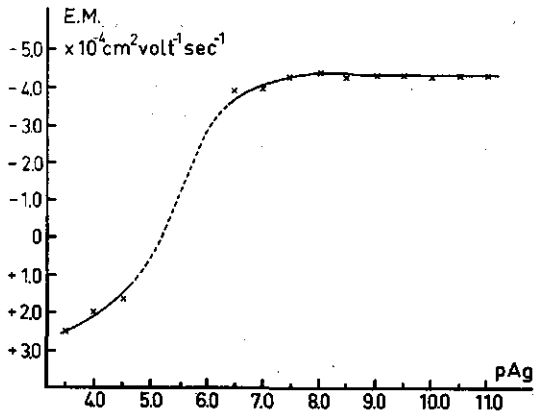

FIGURE 3–1.
Electrophoretic mobility, *E.M.*, of AgI particles as a function of pAg in 10^{-3} *N* KNO_3 solution at 20°C.; $c_{AgI} = 5.10^{-5}$ mole/l; $\varkappa a$ about 7

The results of the measurements given in fig. 3–1, show that the *E.M.* of a negatively charged sol is almost independent of the pAg, even close to the zero point of charge, while the mobility of the positively charged sol decreases gradually on approaching the zero point of charge. As it is not independently known how the graph has to be interpolated between the positive and negative charge region where *E.M.* measurements are impossible because flocculation occurs, the pAg corresponding to the zero point of charge cannot be determined exactly, but will be close to the value of 5.44 given by VAN LAAR (1952).

According to the calculations of WIERSEMA (in which the viscoelectric effect was not taken into account) the maximal value of *E.M.* to be found under the given circumstances amounts to 4.05×10^{-4} $cm^2volt^{-1}sec^{-1}$, which is slightly less than the experimentally observed maximum value of $4.2 \pm 0.1 \times 10^{-4}$ $cm^2volt^{-1}sec^{-1}$. Similar too high values for *E.M.* for AgI sols were found by other investigators (TROELSTRA, 1941; WATANABE, 1960) as is mentioned already by WIERSEMA, who concluded that silver halide sols are not entirely suitable for testing his theory.

When we nevertheless apply WIERSEMA's theory, for ζ a value of at least −125 mV is found, when ψ_0 is as low as about −70 mV (pAg 6.6 relative to pAg 5.4 at the zero point of charge), which is clearly incompatible with current double layer pictures. This discrepancy may imply that as a result of overestimation of the relaxation correction in WIERSEMA's theory the calculated value of ζ is too large, but it is also possible that beside I^- ions negatively charged impurities were adsorbed on the AgI, thus causing the *E.M.* to be higher than it should be. PARFITT and SMITH (1964) sometimes observed velocities at pAg 6 comparable in magnitude with ours. This was accompanied by a shift of the zero point of charge to about pAg 3.5, which implies a considerable increase in ψ_0, so that the large *E.M.* is reasonable again. This shift was ascribed to impurities in the water that was used. As mentioned already, in our case the zero point of charge is close to the pAg value of 5.4 used in the calculation of ψ_0, so that this last quantity will have about the right value.

The influence of relaxation is suppressed when $\varkappa a$ is considerable higher

than 7. Evaluation of ζ is then less complicated, and any observed constancy of *E.M.* with increasing ψ_0 can no longer be ascribed to relaxation effects, and mus be due to viscoelectric influences.

Of course $\varkappa a$ can be raised by increasing either $\varkappa$ or a. Increase of $\varkappa$ can be achieved by increasing the indifferent electrolyte concentration, but the required rise is so large that ζ at the same time drops to such a low value that accurate measurements of *E.M.* can no longer be performed. Increase of a can be achieved by preparing monodisperse sols, as described by EDWARDS, EVANS and LA MER (1962), and OTTEWILL and WOODBRIDGE (1961). These sols consist of particles with a diameter of about 1 μ, corresponding with a $\varkappa a$ value of about 50 in 10^{-3} *N* KNO_3 solution, which is an acceptable value.

OTTEWILL and WOODBRIDGE (1964) have observed that the *E.M.*'s of their monodisperse sols, determined at constant values of the pAg, scatter enormously from one preparation to another. Moreover, the zero point of charge is shifted to about pAg 2, which is much lower than for the more classical sols. Often reversal of charge is not observed, because the zero point of charge is not constant. The maximum experimental values of *E.M.* correspond to a ζ-potential of about –60 mV, which is comparatively low. We could verify the observations of OTTEWILL and WOODBRIDGE qualitatively, and observed the same behaviour with sols prepared according to the method of EDWARDS c.s. (1962).

The behaviour of these monodisperse sols being so capricious they are not suitable for the proposed investigations. This is the more so, because it cannot a priori be ruled out that the relation between surface charge and surface potential is different from that described in chapter 5. As a result of the dilution technique used the AgI concentration in these sols is so low that it is impossible to prepare a sufficient amount of precipitate to apply the adsorption technique and the expected deviation in the charge-potential relation cannot be determined.

Because no other method of AgI sol preparation yielding larger particles is known, we must conclude that at present electrophoretic measurements on AgI sols cannot provide well defined ζ-potentials. Hence, a quantitative test of the LYKLEMA – OVERBEEK theory is not possible with this system.

It is only in order to obtain some qualitative insight therefore, that a few measurements were performed with the small-particle sol in a 10^{-3} *N* KNO_3 solution containing various concentrations of n-butyl alcohol, one of the organic compounds used in the adsorption experiments. The result of these experiments is shown in fig. 3–2. At increasing alcohol concentration the zero point of charge appears to shift to lower pAg values, an effect which will be considered in more detail in chapter 5. At the negative side of the zero point of charge for all alcohol concentrations *E.M.*, as a function of pAg, goes through a maximum, after which it becomes independent of pAg. In table 3–1 it is shown that the magnitude of the *E.M.* in this constant region decreases with the same percentage as the viscosity in solution increases.

Whether the observed constancy is a result of relaxation or of viscoelectric effects cannot be decided, because of the unfavourable $\varkappa a$ value. It is striking, however, that closer to the zero point of charge the *E.M.* is slightly higher than

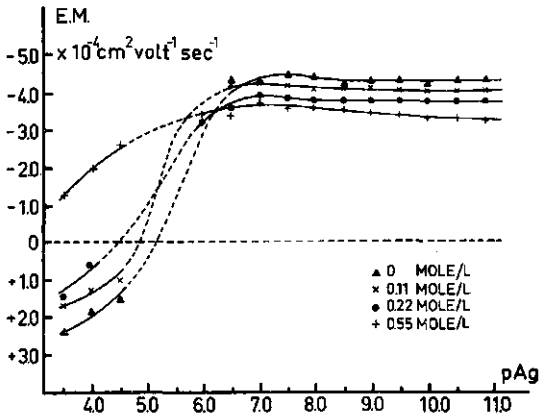

FIGURE 3–2.
Electrophoretic mobility, *E.M.*, of AgI particles as a function of pAg in 10^{-3} *N* KNO_3 solution, containing various concentrations of n-butyl alcohol

in the constant region, which is not predicted by the theories of WIERSEMA and LYKLEMA and OVERBEEK. It may be that discreteness of charge effects (LEVINE and BELL, 1963), are responsible for this aspect, but it should be stressed again that the measurements have only a very qualitative meaning and that a definite answer to these problems cannot yet be given.

TABLE 3–1. Relation between decrease in electrophoretic mobility, and increase in viscosity as a function of alcohol concentration

Concentration n-butyl alcohol in mole/l	% decrease *E.M.*	% increase viscosity
0.11	3.0	3.0
0.22	7.0	7.3
0.55	17.0	18.5

3.3. STREAMING POTENTIAL MEASUREMENTS WITH AgI PLUGS

Streaming potential measurements in general can be performed in two different ways dependent upon the state of the solid material to be investigated. In one method the material constitutes a closed surface in the form of a cylinder of capillary dimensions through which the equilibrium solution is forced; in the other rather finely divided material is pressed together and the solution is forced through the plug thus formed. In both cases the potential difference V arising between the limits of the material is measured as a function of the applied pressure P.

For both systems values of V/P can be converted into ζ-potentials with help of the equation

$$\frac{V}{P} = \frac{\varepsilon \zeta}{4 \pi \eta \lambda} \tag{3-1}$$

in which ε, η, and λ are the dielectric constant, the viscosity and the specific

conductivity of the solution respectively. This equation has been derived on the assumptions that the radii of curvature of the capillary or of the pores in the plug are much larger than the thickness of the double layer, the flow of liquid in the plug is laminar, the conductance is only dependent on the bulk conductivity of the solution, and the viscosity is constant in the whole double layer. Hence, it is questionable to use eq. (3–1) if one or more of these conditions is not fulfilled.

Capillaries with an inner surface consisting of AgI can be made in a reliable way only when the AgI is supported by some conducting material, which makes them unsuitable for streaming potential investigations, where it is essential that conductance takes place in the solution only. Hence the capillary method must be ruled out in the present case. Suitable plugs of AgI particles can easily be made, however, and a set of measurements was accomplished with this technique. The AgI precipitates used in these measurements were the same as those of the titration experiments, which has the advantage that surface charge, surface potential and electrokinetic parameter are determined on exactly the same material in solutions of the same composition. The preparation of these precipitates has been described in chapter 2, together with the streaming potential apparatus used. The applied procedure was essentially the same as described more extensively for the determination of the zero point of charge in chapter 2.

In fig. 3–3 the streaming potential V/P for plugs in equilibrium with 10^{-3} N KNO_3 solution is given as a function of pAg. The zero point of charge can be determined accurately from this graph, because measurements close to this point are possible, which is a definite advantage of this technique as compared with electrophoresis. According to fig. 3–3 the zero point of charge corresponds to pAg = 5.34, which is in good agreement with the value of 5.44 found by VAN LAAR (1952). For negative charges V/P levels off at a value of –4.65 mV/cm Hg, and is constant for pAg values higher than 8.5. In the positive charge region measurements were not extended further than about pAg = 3.5, because the increasing concentration of potential determining ions would lead to a too high

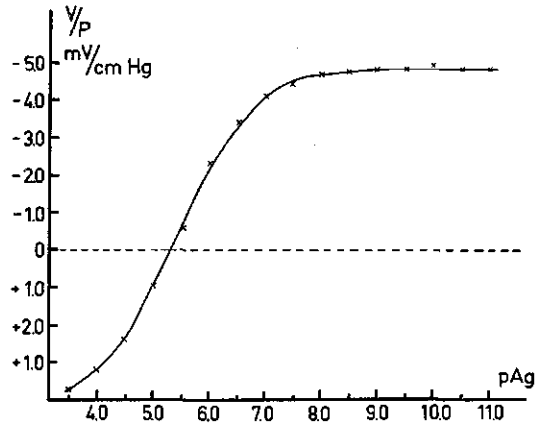

FIGURE 3–3.
Streaming potential, V/P, as a function of pAg for a AgI plug in equilibrium with a 10^{-3} N KNO_3 solution

ionic strength, which in turn would affect the ζ-potential. It is obvious however that the figure is about symmetrical around the zero point of charge.

Before the measured V/P values are converted into ζ-potentials it must be established whether the assumptions made in the derivation of eq. (3–1) are fulfilled in the present system. Under all circumstances V vs. P was a straight line at the rather low pressures applied, so that the flow of liquid was laminar. The value of $\varkappa a$ is difficult to assess; the precipitate particles are visible with the naked eye, so that their diameter will be larger than 1 μ, and $\varkappa a$ exceeds 50. In chapter 5 some evidence is given, however, that these particles may be agglomerates of much smaller entities, so that it is questionable whether the radii of curvature of the pores in the plug are much larger than the thickness of the double layer. The resistance of several plugs was determined after V/P at the corresponding pAg had been measured. 10^{-3} N KNO_3 was then replaced by 10^{-1} N KNO_3 and the resistance measured again, which provides the cell constant (WIJGA, 1946). That the geometry of the plug did not change during this procedure was shown by replacing 10^{-1} N by 10^{-3} N KNO_3 solution again, after which the same resistance was measured as before. The cell constant was then used to calculate the conductivity λ_p of the plug in 10^{-3} N KNO_3. The ratio between this conductivity and the conductivity of a free 10^{-3} N KNO_3 solution, λ_0, measured at the same temperature, is shown in fig. 3–4 as a function of pAg. From this graph it can be seen that the conductivity in the plug is always several percent higher than in the solution, this effect increasing with increasing charge on the AgI. In the zero point of charge the effect must be ascribed to conductance in the solid AgI itself, because surface conductance is presumably absent there. Hence, it is obviously not fully correct to consider AgI as non-conducting, which is a serious drawback of the system because this forms a prerequisite in all derivations of electrokinetic equations. The increase in λ_p/λ_0 at increasing charge must be due to surface conductance, and even when the conductivity in the AgI would be absent, this is serious enough in itself. OVERBEEK and WIJGA (1946) and OVERBEEK and VAN EST (1952) have shown that it is impossible in principle to convert V/P values measured on plugs into ζ-potentials when surface conductance contributes more than a few percent in the total conductivity. Altogether it must again be concluded that it is impossible

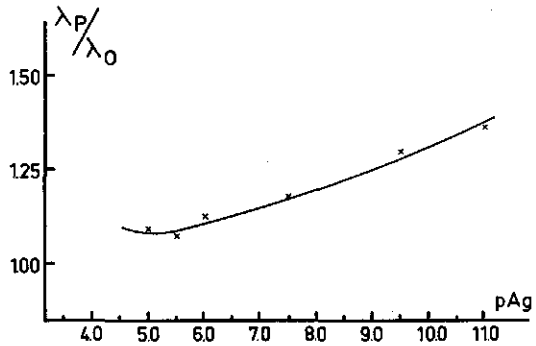

FIGURE 3–4.
Ratio between the conductivity λ_p of a AgI plug in equilibrium with a 10^{-3} N KNO_3 solution, and the conductivity λ_0 of a 10^{-3} N KNO_3 solution, as a function of pAg

to derive ζ-potentials from an electrokinetic phenomenon in the AgI system, and for this reason further investigations were not performed.

Notwithstanding this conclusion it is interesting to calculate ζ-values from the results of fig. 3–3 with the help of eq. (3–1). When λ_0 is substituted in eq. (3–1), the pAg independent maximum V/P value appears to correspond with a constant value of –68 mV for ζ. When λ_p is used, ζ increases slightly with pAg in the constant V/P region and reaches a value of –90 mV at pAg 11.0. This is still considerable lower than the value of –125 mV calculated from the constant *E.M.* at high pAg, but comparable to the ζ-values derived from sedimentation potential measurements by RUTGERS and NAGELS (1958).

It should be remarked yet that the foregoing conclusions do not invalidate the determination of zero points of charge with the help of AgI plugs, for the intersection point of the dV/dP vs. pAg relation with the axis $dV/dP = 0$ is not affected.

CHAPTER 4

THE SPECIFIC SURFACE AREA OF THE SILVER IODIDE SAMPLES, AND THE CHARACTER OF THE SILVER IODIDE CHARGE

Prior to a discussion of the titration results, we must focus our attention on two subsidiary but relevant problems, viz. the determination of the specific surface area of AgI suspensions, and the distribution of charge and potential inside the solid.

4.1. Specific surface area of AgI samples

In chapter 2 it has been discussed that determination of the amount of adsorbed potential determining ions can be used as a starting point of double layer investigations on AgI. This amount of adsorbed ions has then to be converted into a specific surface charge σ ($\mu C/cm^2$), and this can only be accomplished when the specific surface area of the AgI sample is known. The value of this quantity is rather difficult to evaluate unambiguously and constitutes the object of a separate research by VAN DEN HUL. Some methods of surface area determination, such as negative adsorption of co-ions and positive adsorption of gases and dyes, are discussed by VAN DEN HUL and LYKLEMA (1964). As mentioned by them, our titration technique also provides a method for the evaluation of the specific surface area. By differentiation of a $\sigma - E$ graph a differential capacity is obtained, which near the zero point of charge is assumed to be equal to that on mercury, at least at low electrolyte concentration (MACKOR, 1951). At low concentrations the capacity is determined almost completely by the diffuse part of the double layer, at least when there is no specific adsorption, and this capacity should be equal for AgI and mercury. Thus by comparison of the experimentally determined capacity on AgI with the capacity on mercury in KF solutions as given by GRAHAME (1947), the surface area per gram is found. We preferred the use of KNO_3 because this can be obtained more easily in pure form than KF. This procedure is possible because LIJKLEMA (1957) found that KNO_3 and KF gave indistinguishable capacities at the zero point of charge.

In order to check the results of this method with those of the negative adsorption method, employed by VAN DEN HUL, a sample of AgI was divided into two parts. From one part the surface area was determined by negative adsorption of phosphate, which yielded 1.4 ± 0.2 m^2/gram and from the other by the capacity method mentioned above, yielding 1.2 ± 0.1 m^2/gram. After the capacity was measured the area of this part of the sample was also determined by negative adsorption, now giving 1.3 ± 0.2 m^2/gram. Therefore, the agreement is within the experimental error.

For the samples used in the titration experiments the specific surface area, as determined by the capacity method, appeared to be different for each indepen-

dently prepared sample, but was always between 1 and 3 m^2/gram. This is of the same order of magnitude as the values of AGAR (1961) and CORRIN and STORM (1963), but lower than the value of 5.5 m^2/gram given by LIJKLEMA (1957). This difference is probably due to differences in length and circumstances of the ageing process.

Another point of interest with regard to the surface area was the indication from LIJKLEMA's (1957) work that the adsorption per gram decreased with increasing weight of the AgI sample in the same volume of solution. In order to check this an adsorption isotherm was determined with 50 gram AgI in 300 ml. 10^{-1} N KNO_3. When this isotherm was completed the amount of AgI was reduced to 45.1 gram and another isotherm determined, after which the amount was successively further reduced to 32.1, 18.0 and 7.8 gram, all in 300 ml. 10^{-1} N KNO_3. From the isotherms the ratio σ_x/σ_{18} was deduced for several E's. This ratio did not show any systematic change, from which it is concluded that there is no influence of the amount of AgI per given volume of solution on the adsorption per gram, at least not in the range covered by these experiments.

4.2. CHARACTER OF THE AgI CHARGE AND DISTRIBUTION OF THE POTENTIAL DIFFERENCE OVER THE TWO PHASES

In the preceding section it was tacitly assumed that the deficit of potential determining ions in the solution is associated with a *uniform* charge on the surface of the AgI particles. One may wonder whether this uniformity really exists, or whether the adsorption is localized at edges and dislocations. The answer to this question is important in connection with the formulation of the charge distribution in the solution part of the double layer. LYKLEMA and OVERBEEK (1961 b) showed that the STERN–GOUY–CHAPMAN theory, based on a uniformly smeared out charge at the interface, explained their measurements very satisfactorily. Moreover, in the preceding section of this chapter it was shown that determinations of the specific surface area, based on this theoretical concept gave good mutual agreement. On the basis of these considerations we conclude that whatever the character of the AgI charge, it may be treated as being distributed uniformly over the surface. This conclusion is also supported by the observed electrical conductivity in the AgI.

One may also wonder whether the AgI charge is really located at the surface of the particles, or if it constitutes a space charge within the particles. In the appendix to this chapter it is shown that the field strength in the solution is independent of the character of the AgI charge. The character of the AgI charge is important, however, with regard to the distribution of the potential difference between the bulk of AgI and solution respectively, over both phases. MACKOR (1951) has already considered this question, and he assumed that the double layer continued inside the solid phase, as in AgBr (GRIMLEY and MOTT, 1947; GRIMLEY, 1950). His conclusion was that 'the influence of the double layer in solid AgI is probably small'.

However, in MACKOR's analysis it was implicitly assumed that the charge

inside the AgI is made up of SCHOTTKY-defects, while in fact FRENKEL-defects prevail (BURLEY, 1963). This topic will therefore be reconsidered.

The number of FRENKEL-defects per cm^3, n, is given by the relation (KITTEL, 1960)[1]

$$\ln \frac{(N-n)\,(N'-n)}{n^2} = \frac{A}{kT} \tag{4–1}$$

where N is the number of lattice sites and N' the number of interstitial places, both per cm^3, while A is the energy required to bring a Ag^+ ion from a lattice site to an interstitial position. When $n \ll N$ and $n \ll N'$, and when we assume that $N = N'$, eq. (4–1) can be simplified to give

$$n \approx Ne^{-A/2kT} \tag{4–2}$$

which is the same equation as has been used by SHAPIRO and KOLTHOFF (1947).

For the numerical solution of eq. (4–2) we note that N is equal to $2N_{Av.}d/M$, where $N_{Av.}$ is AVOGADRO's number, d is the density of AgI and M is the molecular weight of AgI. Substituting $N_{Av.} = 6.02 \times 10^{23}$, $d = 5.67$ and $M = 234.8$ we find $N = 2.9 \times 10^{22}$ cm^{-3}. As to A, there is no generally accepted value for this parameter in the literature. BURLEY (1963), not quite correctly citing TELTOW (1950), states that A can be of the order of only about 0.1 eV, which is unreasonably low. On the other hand a value of 0.69 eV, based upon both heat conduction measurements and theoretical calculations, has been given by LIESER (1954; 1956). Between these extremes other values are possible, depending upon the mode of preparation of the AgI and the number of foreign atoms incorporated in it (LIESER, 1956).

$A = 0.1$ eV gives $n = 3.9 \times 10^{21}$ cm^{-3} and $A = 0.69$ eV results in $n = 4.9 \times 10^{16}$ cm^{-3}, corresponding with a number of charge carriers in AgI of 7.8×10^{21} cm^{-3} and 9.8×10^{16} cm^{-3} respectively. For AgBr, a similar large spread in n values has been quoted very recently by OTTEWILL and WOODBRIDGE (1964).

According to the theory of the double diffuse double layer of VERWEY and NIESSEN (1939) the potential distribution between two adjacent phases is given by the equation

$$\frac{\sinh y_1}{\sinh y_2} = \sqrt{\frac{n_2\varepsilon_2}{n_1\varepsilon_1}} \tag{4–3}$$

where $y = e\psi/2kT$, while ψ, n and ε refer to the potential drop, the number of charge carriers per cm^3 and the dielectric constant respectively in the phase designated by the subscript. In the present case the subscript 1 refers to the solution and 2 to the AgI.

[1] We are very much indebted to drs. L. BLOK for stimulating discussions on these problems.

Assuming that the STERN layer between the GOUY layer and the surface of the particle is charge-free, eq. (4–3) can be applied with substitution of ψ_δ for ψ_1. With the help of this equation ψ_{AgI} can then be calculated as a function of ψ_δ and of electrolyte concentration, making use of $\varepsilon_{H_2O} = 80$ and $\varepsilon_{AgI} = 13.2$ (JAYCOCK, 1963). Some results to illustrate such calculations, are given in table 4–1, where ΔE denotes the difference between the E values of the charge under consideration and the *z.p.c.* respectively; ΔE is equivalent to the change in GALVANI potential difference between AgI and solution.

As can be seen from table 4–1 values of ψ_{AgI} calculated on the basis of $n_2 = 9.8 \times 10^{16}$ cm^{-3} are very considerable. For high surface charges ψ_{AgI} amounts to as much as 85 % of ΔE, while for $\sigma = -0.25$ μC/cm^2 it even far exceeds ΔE. This last finding being obviously an impossible result, the effect must have been *over*estimated.

TABLE 4–1. Calculation of the potential drop inside AgI as a function of ψ_δ and of electrolyte concentration. Explanation in the text

Electrolyte concentration	σ μC/cm^2	ψ_δ mV	ψ_{AgI} mV		ΔE mV
			$n_2 = 7.8 \times 10^{21}$ cm^{-3}	9.8×10^{16} cm^{-3}	
10^{-3} *N* KNO_3	–0.25	–32	–1	–124	–65
	–2.5	–130	–10	–240	–350
10^{-1} *N* KNO_3	–0.25	–1.4	–0.6	– 80	–18
	–3.5	–46	–16	–260	–306

LIJKLEMA (1957) interpreted his titration experiments with a model in which $\Delta E = \Delta\psi_1$, thus omitting ψ_{AgI}. This model could explain his experimental findings quite satisfactorily, and one is tempted to rely therefore on the relatively small values of ψ_{AgI} found on the basis of $n_2 = 7.8 \times 10^{21}$ cm^{-3}. However, this value of n_2 would mean that about 18 % of the total number of Ag^+ ions in the solid would be interstitial ions, which is very improbable. Consequently ψ_{AgI} is *under*estimated. Hence, it must be concluded that although ψ_{AgI} has to be accounted for and cannot simply be ignored, its exact value cannot be calculated at present. However, it will be between the extremes of table 4–1.

It should be noted at this point that introduction of a variable ψ_{AgI} is not the only improvement to be made yet. There will also be a change in χ potential, the potential originating from e.g. dipole orientation, on charging the interface, and because this change also contributes to ΔE it has to be accounted for. It is not feasible, however, to discuss the influence of this change in χ potential quantitatively, because information about this parameter is scarce. That LIJKLEMA's model worked so well may possibly be due to (partial) compensation of the contributions of ψ_{AgI} and χ. Anyhow, the present investigations also indicate that the assumption $\Delta E = \Delta\psi_1$ is very reasonable. It must be realized, however, that in principle a splitting of ΔE into its components is somewhat arbitrary, and hence we will present our titration results in the next chapter as

σ versus E curves, as this is a prerequisite for the thermodynamic analysis to be given.

APPENDIX

ABSENCE OF INFLUENCE OF THE CHARGE DISTRIBUTION INSIDE AgI ON THE ELECTRICAL FIELD STRENGTH IN SOLUTION

According to the theory of electrostatics the surface integral of the normal component of the dielectric displacement, D_n, taken over any arbitrarily chosen closed surface S is equal to the charge Q in the volume enclosed by this surface:

$$\oint D_n dS = Q \tag{4–4}$$

For the closed surface S we choose a cylinder of 1 cm^2 cross-section perpendicular to the AgI-solution interface (see fig. 4–1). One plane of this cylinder is situated so far inside the AgI that there is no potential gradient across it. The other plane, S_e, parallel to the interface, is situated in the solutionpart of the double layer at some non-specified distance from the solid. Obviously it is only this plane that contributes to $\oint D_n dS$, and because D_n is equal to $\varepsilon(d\psi/dx)_{sol.}$, where ε = dielectric constant and $(d\psi/dx)_{sol.}$ = electrical field strength in solution, we find

$$\varepsilon\left(\frac{d\psi}{dx}\right)_{sol.} = Q \tag{4–5}$$

When S_e is situated in the charge-free part of the STERN layer eq. (4–5) reduces to

$$\varepsilon\left(\frac{d\psi}{dx}\right)_{\text{STERN layer}} = \sigma \tag{4–6}$$

Equations (4–5) and (4–6) both demonstrate that the field strength in solution is determined by the *value* of the AgI charge, but *not* by its *character*.

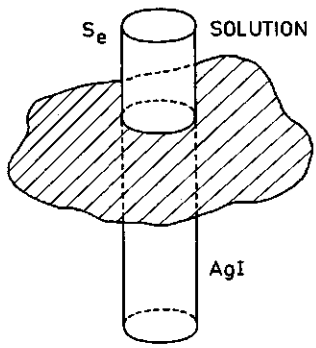

FIGURE 4–1. Cylinder of 1 cm^2 cross-section, perpendicular to the AgI-solution interface. Explanation in the text.

CHAPTER 5

THE DOUBLE LAYER ON SILVER IODIDE IN THE PRESENCE OF NEUTRAL ORGANIC MOLECULES

5.1. Experimental results

5.1.1. *Adsorption isotherms*

In chapter 1 it was explained that double layer investigations on AgI in the presence of neutral organic compounds serve two purposes: a. a comparison with similar investigations on mercury can be made, from which the influence of the charge carrier on the results can be deduced; b. the results may be combined with electrokinetic measurements in an attempt to gain more insight into the principles underlying the slipping process in electrokinetics.

It was expected that thiourea, a compound studied extensively in the mercury system (Schapink, Oudeman, Leu and Helle, 1960; Parsons, 1961), would also be adsorbed strongly on AgI. The study of the adsorption of this compound would be attractive because adsorption changes the double layer characteristics, so that at least one of the purposes would be served. The presence of thiourea in solution, however, caused a considerable lowering of the Ag^+ concentration, due to the formation of a complex between thiourea and Ag^+ ions (Fyfe, 1955). The Ag^+ ions withdrawn from the solution are distributed then among complex and the AgI surface. This distribution cannot be calculated with sufficient accuracy, thus making an analysis in terms of surface charge impossible.

Because this complex formation is highly favoured by the S-atom in the molecule, urea itself was then considered. Complex formation, although not absent, appeared to be much smaller with this compound, and hence titrations were performed in the presence of various concentrations of urea in swamping electrolyte (10^{-1} N KNO_3 solution). The indifferent electrolyte concentration was purposely chosen to be so high because the measured capacity is almost equal then to the capacity of the Stern layer, while the potential drop over this layer is almost equal to the total potential drop in the double layer.

The results of these titrations are shown in fig. 5–1. From these results it can be seen that at constant E, the AgI charge becomes more positive with increasing urea concentration. This is accompanied by a shift in the zero point of charge to a more negative E, corresponding to a higher pAg in the solution. Although these effects are very pronounced, the urea concentrations used are rather high. The properties of the solution change markedly at these high concentrations and e.g. the change in activity coefficient begins to play an important rôle, resulting in a reduced degree of accuracy of the $\sigma - E$ graphs. Because it is attractive to study the influence of added compounds over the whole accessible potential range, the small activity of urea in the negative charge region is another drawback of the system. Furthermore, it seems that urea has not been investigated in the mercury system.

For these reasons other compounds were examined, and it appeared that the

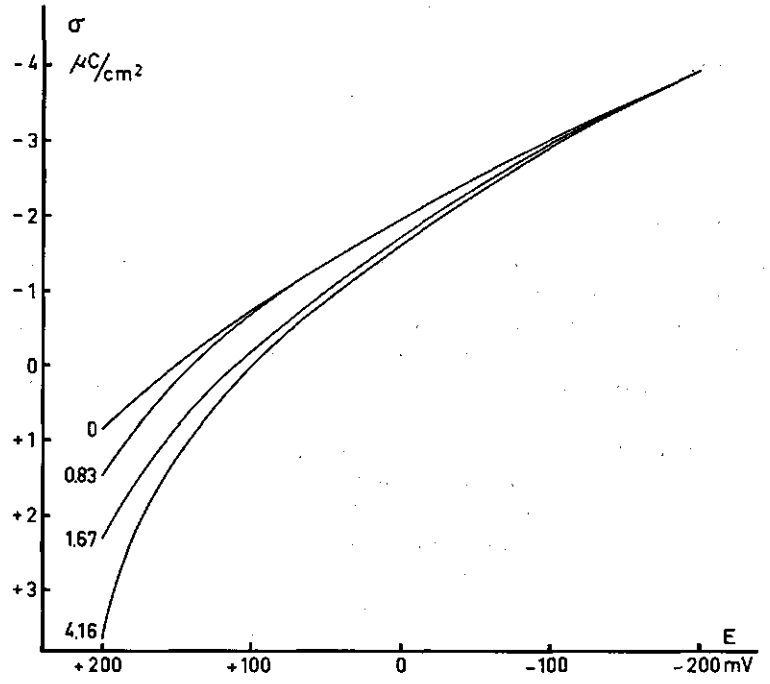

FIGURE 5–1. Surface charge, σ, as a function of cell-EMF, E, for various concentrations (mole/l) of urea. $c_{KNO_3} = 10^{-1}\ N$

monohydric alcohols meet our requirements. The alcohols investigated were: n-propyl-, n-butyl-, n-amyl-, isobutyl-, sec. butyl- and tert. butyl alcohol.

In general experiments could be performed without difficulties, although it should be mentioned that in the presence of tert. butyl alcohol equilibration was rather slow, while the results are not as unambiguous as with the remaining compounds. Only with n-amyl alcohol could reproducible and reliable results not be obtained, because equilibrium was not attained or only very slowly.

The $\sigma - E$ relations for n-butyl alcohol as a function of its concentration in a $10^{-1}\ N$ KNO_3 solution are given in fig. 5–2. For the other alcohols these relations are given on a somewhat reduced scale in the figures 5–3 up to 5–6. Fig. 5–7 shows the same relations for n-butyl alcohol in a $10^{-3}\ N$ KNO_3 solution. For the sake of clarity only about half the number of investigated concentrations is given. Experimental points are omitted since they never differed more than 0.04 μC/cm² from the curve, which is only slightly more than the line width.

These figures show that on addition of alcohol to the base solution the negative charge decreases at cell-EMF's more negative than a characteristic $E = E_m$, while at E's more positive than E_m the charge becomes more negative. The higher the alcohol concentration the more pronounced are these effects. A shift of the zero point of charge to lower pAg values (i.e. to the positive side) at increasing alcohol concentration is also observed. At the cell-EMF $E = E_m$,

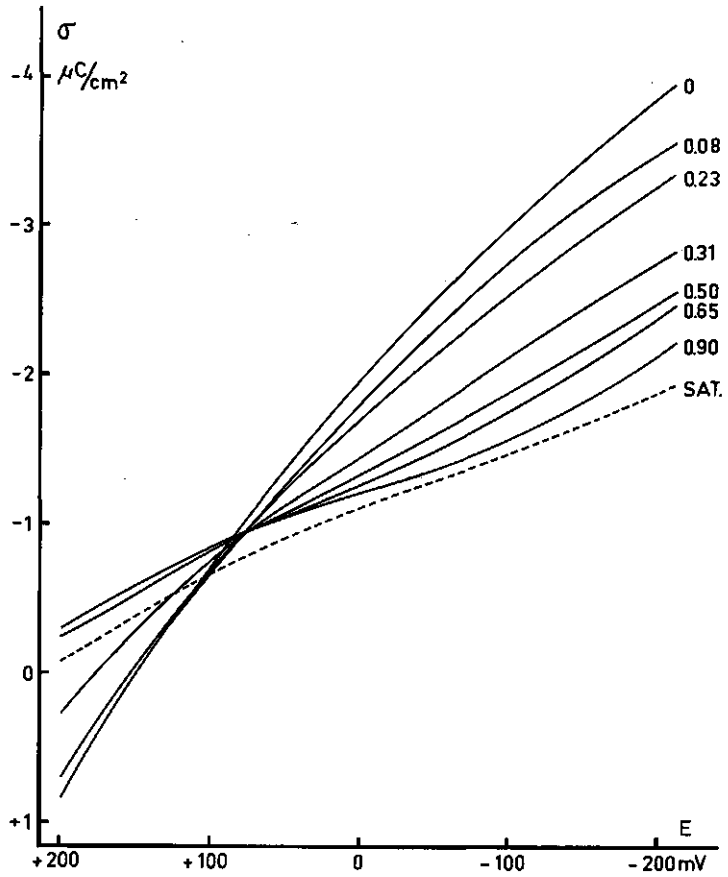

FIGURE 5–2. Surface charge, σ, as a function of cell-EMF, E, for various concentrations (mole/l) of n-butyl alcohol. $c_{KNO_3} = 10^{-1}$ N

σ is unaffected by the alcohol concentration, leading to a common intersection point for all concentrations of a given alcohol. There is only one exception to this common trend. The curves for saturated solutions of n-butyl-, iso-butyl- and sec. butyl alcohol follow quite a different pattern, characterized by smaller negative charges over the largest part of the E range (dashed curves in figures 5–2, 5–4 and 5–5). It is interesting to note that the alcohols behave in quite a different manner from urea.

Although qualitatively the behaviour of all alcohols is the same, it can be seen that the concentration required to reach the same charge depression is different for every alcohol i.e. not every alcohol is equally effective. The charge, σ_m, and the cell-EMF, E_m, of the common intersection point are also different for the individual alcohols, as is shown in table 5–1.

For n-butyl alcohol σ_m is not very much different for 10^{-1} N and 10^{-3} N

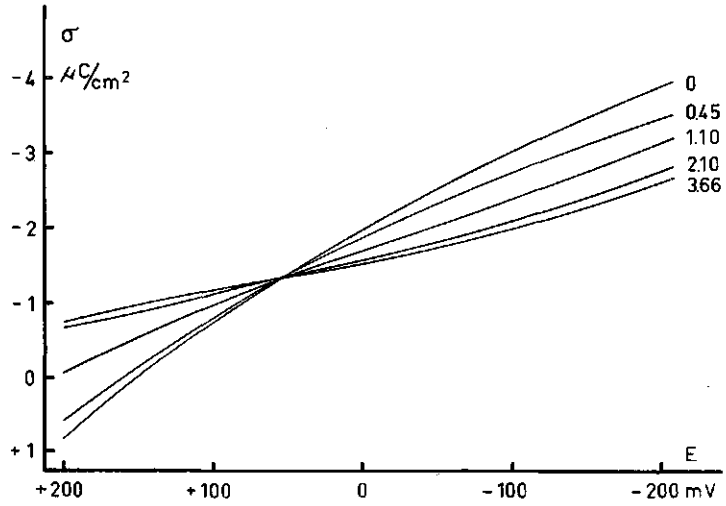

FIGURE 5–3. Surface charge, σ, as a function of cell-EMF, E, for various concentrations (mole/l) of n-propyl alcohol. $c_{KNO_3} = 10^{-1}\ N$

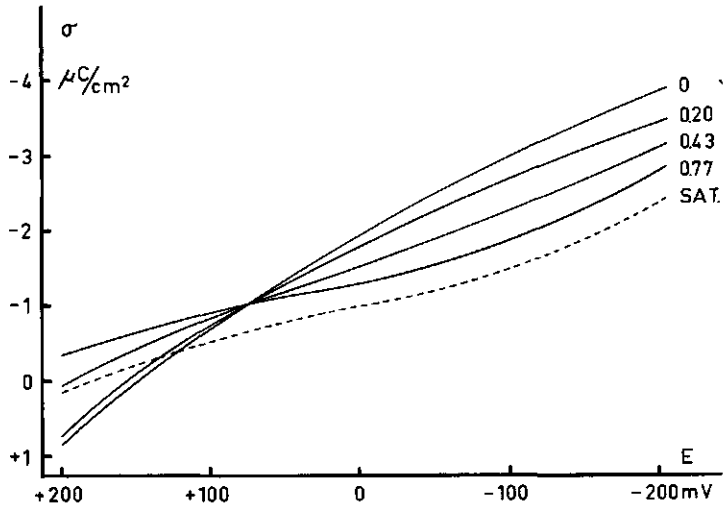

FIGURE 5–4. Surface charge, σ, as a function of cell-EMF, E, for various concentrations (mole/l) of iso-butyl alcohol. $c_{KNO_3} = 10^{-1}\ N$

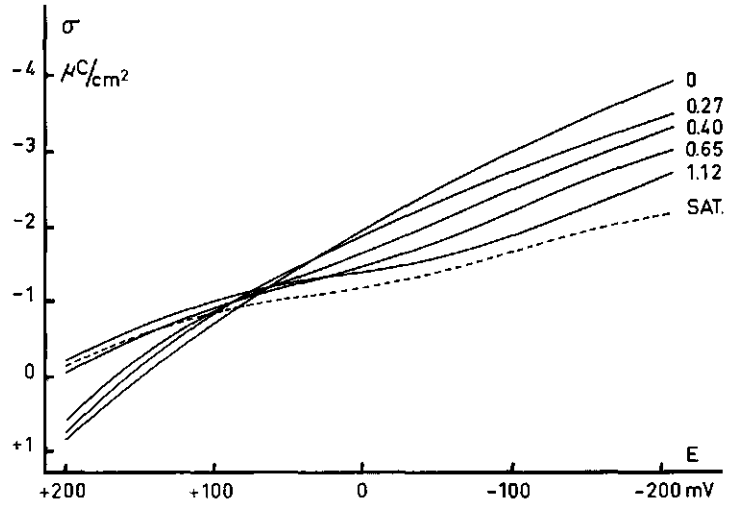

FIGURE 5–5. Surface charge, σ, as a function of cell-EMF, E, for various concentrations (mole/l) of sec. butyl alcohol. $c_{KNO_3} = 10^{-1}\,N$

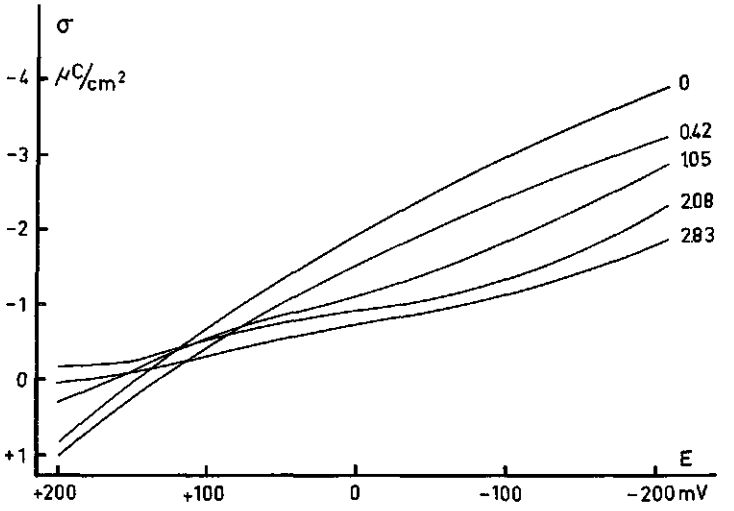

FIGURE 5–6. Surface charge, σ, as a function of cell-EMF, E, for various concentrations (mole/l) of tert. butyl alcohol. $c_{KNO_3} = 10^{-1}\,N$

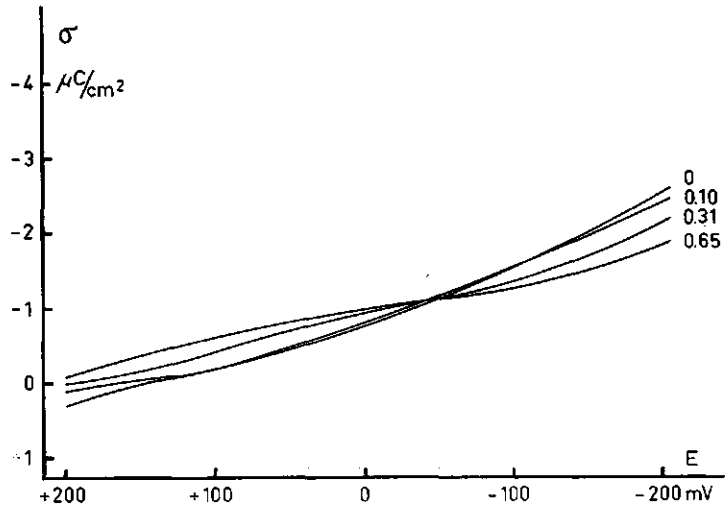

FIGURE 5–7. Surface charge, σ, as a function of cell-EMF, E, for various concentrations (mole/l) of n-butyl alcohol. $c_{KNO_3} = 10^{-3}$ N

KNO_3, but the difference in E_m amounts to about 120 mV. With respect to this difference it should be realized that in 10^{-3} N KNO_3 a large part of the total potential drop takes place across the diffuse part of the double layer. Using the GOUY-CHAPMAN double layer theory, assuming absence of specific adsorption, this contribution is calculated to be 90 mV. Thus the potential drops across the inner part of the double layer are comparable in solutions of different *IEC*.

Comparison of the results of fig. 5–2 on AgI with the corresponding ones on mercury (BLOMGREN, BOCKRIS and JESCH, 1961) in the case of n-butyl alcohol reveals that qualitatively the same behaviour is observed in both systems. The differences between the Hg and the AgI system are quantitative rather than qualitative e.g. the concentrations needed for an equal effect on the charge are smaller on Hg than on AgI.

For mercury the common intersection point in a 10^{-1} N HCl solution is situated at a cell-EMF about 70 mV negative to the $E_{z.p.c.}$ of the base solution, which is close to the value of 80 mV negative to $E_{z.p.c.}$ on AgI in 10^{-1} N KNO_3

TABLE 5–1. Coordinates of the common intersection points in the $\sigma - E$ graphs for different alcohols

Alcohol	10^{-1} N KNO_3		10^{-3} N KNO_3	
	E_m mV	σ_m μC/cm²	E_m mV	σ_m μC/cm²
n-propyl	+53	−1.32		
n-butyl	+70	−1.05	−53	−1.10
iso-butyl	+75	−1.02		
sec.butyl	+50	−1.35		
tert.butyl	ca. +90	ca. −0.80		

solution. The surface charge at this point, however, amounts to about −2.15 $\mu C/cm^2$, which is twice as high as that on AgI. The intersection point corresponds to a negative surface charge in both systems irrespective of its magnitude. It is interesting to note that BLOMGREN et al. and HANSEN, KELSH and GRANTHAM (1963) observed intersection points at positive surface charges in the presence of neutral aromatic compounds (like phenol), which means that in those cases the zero point of charge is shifted towards more negative potentials. From fig. 5–1 a similar shift is deduced for urea on AgI. The behaviour of those substances on mercury therefore resembles in this respect more that of urea on AgI than that of the alcohols.

During the performance of the experiments it was observed that at increasing alcohol concentration the initially rather coarse AgI precipitate gradually grew finer and finer. This effect was accompanied by a notable repeptization of the particles when they were highly negatively charged. One may wonder whether the specific surface area of the precipitate does not change as a result of this diminution, but we presume that this is not the case. In favour of this argument is the fact that the precipitate regains its original appearance when at the end of an experimental series the alcohol is carefully washed away. Moreover the $\sigma - E$ graph for the base solution determined then is exactly the same as at the beginning of the series. This phenomenon may be explained by assuming that the primary particles form loosely packed aggregates in the base solution. They are separated by the action of an alcohol, but because the original packing is loose this process does not change the specific surface area.

5.1.2. *Zero points of charge*

In principle, the shift of the zero point of charge, $\Delta E_{z.p.c.}$, as a function of alcohol concentration can be derived from the $\sigma - E$ curves of the preceding section. In practice, however, difficulties are encountered in this process, because $E_{z.p.c.}$ is beyond the accessible E-range of the $\sigma - E$ curves for the largest part of the concentration range, whereas the $E_{z.p.c.}$ values obtained in the accessible concentration range are too inaccurate. Hence, $\Delta E_{z.p.c.}$ was measured as a function of alcohol concentration for all alcohols investigated, including n-amyl alcohol, by the streaming potential technique described in chapters 2 and 3. Solutions were 10^{-3} N KNO_3 instead of 10^{-1} N, as in the titration experiments, because the streaming potentials are too low to be measured accurately at high electrolyte concentration. The $E_{z.p.c.}$ in the base solution is almost independent of electrolyte concentration, and it is assumed, therefore, that the shift due to the adsorption of alcohol in 10^{-1} N solution is the same as in 10^{-3} N solution.

In fig. 5–8 the results of these measurements are presented for all alcohols as $\Delta E_{z.p.c.}$ vs. concentration. It will be clear that $\Delta E_{z.p.c.} = 58$ mV corresponds with $\Delta pAg = 1$. The shift is always in the direction of lower pAg values, as has been mentioned already in the preceding section. MACKOR (1951) observed a similar behaviour for acetone. For urea $\Delta E_{z.p.c.}$ vs. concentration has not been determined.

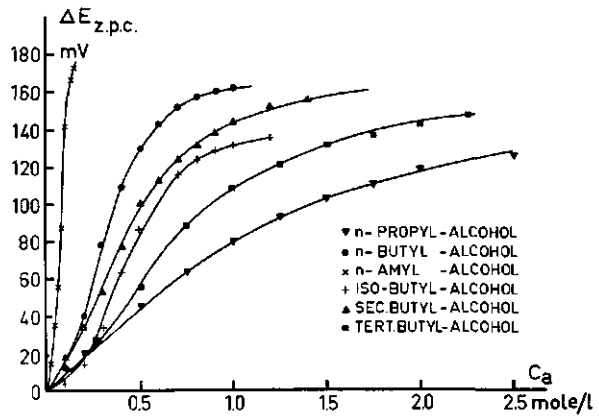

FIGURE 5–8.
Shift of the potential of the zero point of charge, $\Delta E_{z.p.c.}$, as a function of alcohol concentration, c_a, in 10^{-3} N KNO_3 solution, for all alcohols investigated

The shape of the $\Delta E_{z.p.c.}$ curves is not the same for all alcohols. Some (like n-butyl alcohol) show a small increase in $\Delta E_{z.p.c.}$ at low concentrations, but a higher increase at higher concentrations, thus leading to an inflection point. At still higher concentrations the curve levels off, so that the figure is S-shaped. Other alcohols however (like n-propyl alcohol) show a $\Delta E_{z.p.c.}$-concentration relation without an inflection point, resembling a LANGMUIR isotherm. In table 5–2 the types of the $\Delta E_{z.p.c.}$ vs c_a relations are listed together with the experimentally observed maximum shift. For reasons of comparison the corresponding electrophoretically determined characteristics for acetone, deduced from the work of MACKOR (1951), are also included.

TABLE 5–2. Characteristics of the $\Delta E_{z.p.c.}$-alcohol concentration relation, as derived from fig. 5–8

Compound	Type of shift	Observed maximum shift
n-propyl alc.	LANGMUIR	130 mV
n-butyl alc.	S-shape	161 mV
iso-butyl alc.	S-shape	135 mV
sec. butyl alc.	slightly S-shape	157 mV
tert. butyl alc.	slightly S-shape	155 mV
n-amyl alc.	S-shape	ca. 175 mV
acetone	LANGMUIR	ca. 185 mV

Although the maximum shift is different for different alcohols the mutual differences do not amount to more than 30 %, whereas the alcohol concentrations required to reach the maximum differ by as much as a factor 20. With respect to the maximum shifts it is noteworthy again that from the work of BLOMGREN et al. (1961) for n-butyl alcohol in the mercury system a maximum shift in $E_{z.p.c.}$ of 240 mV can be deduced, and that this value is reached much more rapidly as a function of alcohol concentration than in the AgI system.

5.2. Discussion

5.2.1. *Thermodynamics of the adsorption*

The qualitative similarity between the $\sigma - E$ curves on mercury and those on AgI in the presence of n-butyl alcohol strongly suggests a similarity in the adsorption determining parameters in both systems. The adsorption characteristics (e.g. the Gibbs free energy of adsorption) on mercury being known, we can check the suggested analogy if we are able to evaluate the equivalent parameter for the AgI system. In principle this can be accomplished in two different ways, viz. by thermodynamic means and with the help of model considerations.

We will first analyse our adsorption isotherms thermodynamically. For that purpose the Gibbs equation is applied to the AgI-solution interface (Overbeek, 1952; Agar, 1961):

$$d\gamma = -\sum_{\substack{\text{neutral}\\ \text{compounds}}} \Gamma_i d\mu_i - \sigma\, dE_s - \sum_{\substack{\text{ionic}\\ \text{compounds}\\ i \neq Ag,I}} \Gamma_i d\mu_i \qquad (5\text{–}1)$$

γ = Gibbs free energy of 1 cm^2 of the interface
Γ_i = surface excess of component i per cm^2
μ_i = chemical potential of component i
E_s = potential difference between AgI and solution

The terms $\Gamma_{H_2O}\, d\mu_{H_2O}$ and $\Gamma_{KNO_3}\, d\mu_{KNO_3}$, included in eq. (5–1), can be neglected because they can be shown to be small compared with $\Gamma_{alc.} d\mu_{alc.}$. Since, moreover, $dE_s = dE$, eq. (5–1) can be simplified to give

$$d\gamma = -\Gamma_a d\mu_a - \sigma dE \qquad (5\text{–}2)$$

with the subscript a referring to the alcohol.

By cross-differentiation of eq. (5–2) and subsequent integration we find, substituting alcohol concentrations for activities

$$(\Gamma_a)_{E_2} - (\Gamma_a)_{E_1} = \frac{1}{RT} \int_{E_1}^{E_2} \left(\frac{\delta\sigma}{\delta ln\, c_a}\right)_E dE \qquad (5\text{–}3)$$

where E_1 and E_2 are arbitrarily chosen values of E.

We relate the adsorption at any cell-EMF (E_2) to the adsorption at the cell-EMF of the common intersection point ($E_1 = E_m$). Since $\delta\sigma/\delta ln\, c_a$ is zero at $E = E_m$, while

$\int_{E_m}^{E_2} \left(\frac{\delta\sigma}{\delta ln\, c_a}\right)_E dE$ is always negative, the resulting equation

$$(\Gamma_a)_{E_2} - (\Gamma_a)_{E_m} = \frac{1}{RT} \int_{E_m}^{E_2} \left(\frac{\delta\sigma}{\delta ln\, c_a}\right)_E dE \qquad (5\text{–}4)$$

describes the *desorption* of alcohol with respect to the intersection point. This implies that the adsorption on AgI is maximum at the intersection point. BLOMGREN et al. (1961) showed by a direct thermodynamic analysis of their surface tension data that the same holds on mercury. In view of the similar $\sigma - E$ curves in both systems the present result could be expected.

By graphical analysis of the figures 5–2 to 5–7 on the basis of eq. (5–4) the desorption of the alcohols, relative to their adsorption maximum, was determined as a function of E and the alcohol concentration c_a in 10^{-1} N KNO_3 solutions. The result of this analysis for n-butyl alcohol is given in fig. 5–9, where the adsorption maxima for all concentrations are made to coincide, because absolute values of Γ cannot be determined at this point (nor at any other; see sections 5.2.2. and 5.2.3.). The desorption curves for the other alcohols are qualitatively the same in view of their similar $\sigma - E$ curves, although there are quantitative differences.

The most striking feature of fig. 5–9 is the pseudoparabolic form of the desorption curves. Furthermore it can be seen that for any given potential $E < E_m$ the desorption first increases upon increase of the n-butyl alcohol concentration, but later on ($c_a > 0.4$ mole/l) decreases. A similar behaviour is shown by n-propyl- and sec. butyl alcohol where the 'inversion' concentrations are 1.25 and 0.50 mole/l respectively. With iso-butyl alcohol on the contrary the desorption is an ever increasing function of the concentration until saturation of the solution is reached. For tert. butyl alcohol no definite conclusion can be drawn because the analysis for that compound breaks down at $c_a = 1.50$ mole/l. Up to this concentration however the trend is the same as for iso-butyl alcohol.

At potentials $E > E_m$ the desorption of n-butyl alcohol is less dependent upon E than at $E < E_m$; the inversion concentration here is 0.30 mole/l. The corresponding inversion concentrations for n-propyl-, iso-butyl- and sec. butyl

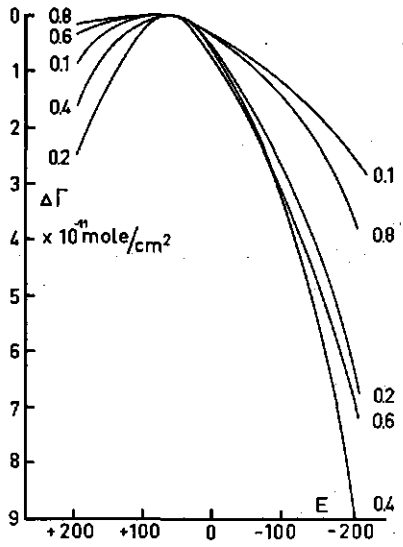

FIGURE 5–9. Desorption of n-butyl alcohol, $\Delta\Gamma$, relative to the adsorption maximum, as a function of the cell-EMF, E, for different concentrations (mole/l). $c_{KNO_3} = 10^{-1}$ N

alcohol are 0.85, 0.50 and 0.30 mole/l respectively. It is noteworthy that isobutyl alcohol has an inversion point for $E > E_m$ but not for $E < E_m$.

Desorption curves for n-butyl alcohol on mercury show the same pseudo-parabolic behaviour as those of fig. 5–9 and they also are flatter at the positive side of the adsorption maximum. Moreover, they also show inversion concentrations. Quantitatively the effects on mercury are more pronounced, e.g. a lower alcohol concentration suffices to reach the same desorption. As an illustration of this we mention that the desorption curves for 0.7 mole/l n-butyl alcohol on AgI and for 0.1 mole/l on mercury are identical over the whole potential range, provided E is referred to E_m in both cases.

In order to apply eq. (5–3) to the $\sigma - E$ curves of urea (fig. 5–1) we substitute $E_c = E_1$, where E_c is some cell-EMF at high negative surface charge, where all $\sigma - E$ curves coincide. For $E < E_c$ we find $\delta\sigma/\delta ln\ c = 0$, which implies that Γ_{urea} = constant (and presumably zero). For $E > E_c$ the integral

$\int_{E_c}^{E_2} \left(\frac{\delta\sigma}{\delta ln\ c}\right) dE$ is positive however, which means that the adsorption increases

with increasing positive E. This effect is the more pronounced the more concentrated is the urea solution. That urea has a higher affinity for positive than for negative AgI is not surprising in view of the tendency of Ag^+ ions to form complexes with urea in solution. It is not impossible, therefore, that we deal here with chemisorption rather than with physical adsorption.

5.2.2. *GIBBS free energy of adsorption*

For conversion of the calculated desorption values into absolute surface excesses one needs a potential range wide enough to arrive at complete desorption. The accessible potential range for AgI (about 400 mV) is far too small to fulfil this requirement. Hence, absolute surface excesses cannot be found by the thermodynamic analysis of the preceding section. However, the introduction of assumptions about the desorption curves in the non-accessible range can give information about the adsorption, where we can take advantage of the analogy with mercury.

DEVANATHAN (1962) has shown that for constant values of the surface charge the adsorption of n-butyl alcohol on mercury is given by a LANGMUIR type isotherm, which can be written in the form

$$\frac{\theta}{1-\theta} = \frac{c_a}{55.5} \exp\left(-\frac{\Delta G_0 + \Delta G_{el.}}{RT}\right) \qquad (5\text{–}5)$$

θ = degree of coverage of the surface by alcohol. The GIBBS free energy of adsorption, ΔG, has been split up into a 'chemical part' ΔG_0, and an 'electrical' part $\Delta G_{el.}$.

When we assume that the identity of the desorption curves for 0.7 mole/l n-butyl alcohol on AgI and 0.1 mole/l on mercury holds also beyond the available desorption region until desorption is complete, which is equivalent to the assumption that the variation of $\Delta G_{el.}$ with E is equal in both systems, we can say that the adsorption is equal over the whole potential range, and that on AgI a LANGMUIR isotherm also applies. ΔG for Hg being known, we then have a method to calculate ΔG for adsorption on AgI, because

$$\frac{\theta}{1-\theta} = \frac{0.7}{55.5} \exp\left(-\frac{\Delta G}{RT}\right)_{AgI} = \frac{0.1}{55.5} \exp\left(-\frac{\Delta G}{RT}\right)_{Hg}$$

The value of ΔG_{AgI} at the adsorption maximum is thus found to be -3.1 ± 0.2 kcal/mole, based on $\Delta G_{Hg} = -3.9 \pm 0.1$ kcal/mole (DEVANATHAN, 1962). The factor 7 used was roughly verified for other combinations of concentrations (by interpolation of the Hg and AgI data).

The same procedure as described above was applied to the other alcohols, where the now available value of ΔG_{AgI} for n-butyl alcohol was taken as the reference. This means that the concentrations of n-butyl alcohol and the alcohol under consideration having the same desorption curves were evaluated. The ΔG values thus found are compiled in table 5–3. A discussion of these values will be given later. For the moment suffice it to note that the observed differences between mercury and silver iodide are reduced to a difference in adsorption energy in both systems.

TABLE 5–3. GIBBS free energy of adsorption, ΔG, for the five alcohols investigated, derived with the help of a model described in the text

Alcohol	$-\Delta G$ kcal/mole
n-propyl	2.2
n-butyl	3.1
iso-butyl	3.4
sec.butyl	3.0
tert.butyl	2.2

5.2.3. *Adsorption of alcohols as evaluated by application of model considerations*

In section 5.2.1. it has been shown that thermodynamic analysis of the $\sigma - E$ curves reveals interesting analogies between Hg and AgI. However, a drawback of this analysis is that it cannot yield absolute adsorption values. These values cannot be found by a direct experiment either. The surface area of the AgI samples is so small that even with a large amount of AgI, alcohol adsorption corresponds to unmeasurable variations in the (relatively large) alcohol concentration in solution. Therefore, in the following sections attempts are made to derive adsorption values from the experimental results by application of model

considerations. These models successively apply to three different conditions of the surface charge.

5.2.3.1. Adsorption of alcohols at the zero point of charge

A layer of molecules adsorbed at an interface gives rise to a potential difference χ across this layer. χ is related to the properties of the adsorbed molecules by the HELMHOLTZ equation

$$\chi = \frac{4\pi n \mu}{\varepsilon} \tag{5-6}$$

where

n = number of adsorbed molecules per cm^2

μ = component of the dipole moment of adsorbed molecules perpendicular to the interface

ε = dielectric constant of the adsorbed layer of molecules

The experimentally determined changes in $E_{z.p.c.}$ (fig. 5–8) are equal to the changes in this χ-potential upon alcohol adsorption. As in this process adsorbed water molecules are replaced by alcohol molecules

$$\Delta E_{z.p.c.} = 4\pi \left(\frac{\mu_w}{\varepsilon_w} \Delta n_w + \frac{\mu_a}{\varepsilon_a} \Delta n_a \right) \tag{5-7}$$

where the subscripts w and a refer to water and alcohol respectively, and Δ denotes the change in a parameter. The exact number of water molecules leaving the surface upon adsorption of one alcohol molecule, b, is not known beforehand, but there is no need to specify it. It will only be assumed that it does not depend upon the total number of alcohol molecules to be adsorbed. Under these circumstances $\Delta n_w = b\Delta n_a$, with b as a constant. Eq. (5–7) can be written then

$$\Delta E_{z.p.c.} = 4\pi \Delta n_a \left(b \frac{\mu_w}{\varepsilon_w} + \frac{\mu_a}{\varepsilon_a} \right) \tag{5-8}$$

If we assume, moreover, that μ_w/ε_w and μ_a/ε_a do not depend upon the amount of alcohol adsorbed, eq. (5–8) can be rearranged to give

$$\Delta n_a = \text{constant.}\ \Delta E_{z.p.c.} \tag{5-9}$$

Eq. (5–9) implies that the curves of fig. 5–8 can be interpreted as adsorption isotherms for the alcohols at the zero point of charge. Hence it is worthwhile to consider these curves in more detail, the qualitative aspects being given already in table 5–2.

With respect to the appearance of the present isotherms for the four isomeric butyl alcohols, it is noteworthy that they are comparable with the adsorption

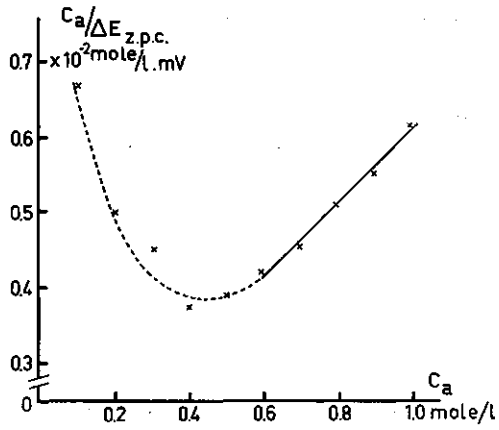

FIGURE 5–10.
Ratio of alcohol concentration, c_a, and related shift in the potential at the zero point of charge, $\Delta E_{z.p.c.}$, as a function of c_a, for n-butyl alcohol

isotherms for adsorption of these alcohols from the vapour phase on graphitized carbon black (AVGUL', KISELEV and LYGINA, 1961). The next point of interest is whether the curves are of the LANGMUIR type (when indicated as such in table 5–2) and whether they can be described by a LANGMUIR type equation at the higher concentrations despite an inflection point at lower coverages.

If the LANGMUIR isotherm is valid, the relation

$$\frac{c_a}{\Delta E_{z.p.c.}} = \frac{1}{k_1} + \frac{c_a}{\Delta E_{z.p.c.}{}^{max}} \qquad (5\text{–}10)$$

has to be fulfilled, where k_1 = a constant and $\Delta E_{z.p.c.}{}^{max}$ = the maximum value of $\Delta E_{z.p.c.}$ obtainable.

When plotted as a function of c_a (for an example see fig. 5–10) $c_a/\Delta E_{z.p.c.}$ gave straight lines for all alcohols, at least when the concentration in solution was higher than a given critical value $c_a{}^l$, which is different for different alcohols. Below this concentration $c_a{}^l$ the points form a strongly curved line, except in the case of n-propyl alcohol where below $c_a{}^l$ another straight line with a slightly different slope was found, and n-amyl alcohol where no straight line existed at all. From the slope of the straight lines $\Delta E_{z.p.c.}{}^{max}$ was evaluated. Values of this parameter, together with values of $c_a{}^l$ are tabulated in table 5–4.

TABLE 5–4. Characteristics of the adsorption isotherms at the zero point of charge. Explanation in the text

Alcohol	c_a mole/l	$\Delta E_{z.p.c.}{}^{max}$ mV	$-\Delta G$ kcal/mole
n-propyl	1.3	189	2.3 $c_a < c_a{}^l$ 2.2 $c_a > c_a{}^l$
n-butyl	0.6	192	3.2
iso-butyl	0.8	161	3.2
sec.butyl	0.6	240	2.6
tert.butyl	1.2	221	2.3

FIGURE 5–11.
Degree of surface coverage at the zero point of charge, $\theta_{z.p.c.}$, as a function of alcohol concentration, c_a, for n-butyl alcohol

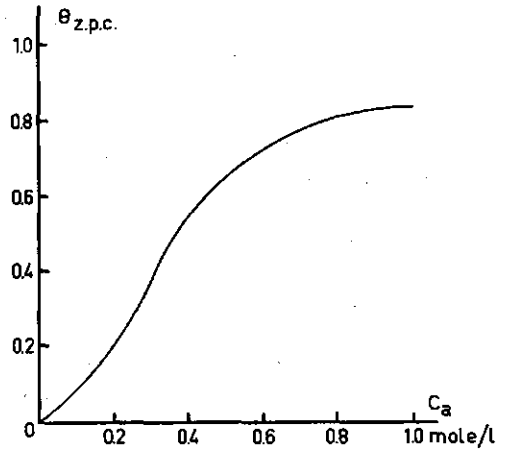

Having now at our disposal $\Delta E_{z.p.c.}{}^{max}$ we can calculate the degree of surface coverage $\theta_{z.p.c.}$ at the zero point of charge as a function of c_a, $\theta_{z.p.c.}$ being equal to $\Delta n_a/\Delta n_a{}^{max}$ and according to eq. (5–9) this is equivalent to saying $\theta_{z.p.c.} = \Delta E_{z.p.c.}/\Delta E_{z.p.c.}{}^{max}$.

By way of example, in fig. 5–11 $\theta_{z.p.c.}$ is given for n-butyl alcohol. As a matter of course this figure has the same appearance as the related $\Delta E_{z.p.c.}$–c_a relation (fig. 5–8). One can then predict the $\theta_{z.p.c.}$–c_a relations for the other alcohols. It is a noteworthy feature of fig. 5–11 that the surface is not yet completely covered with adsorbate when the alcohol concentration in solution reaches saturation (1.05 mole/l.) KIPLING (1963) concluded the same behaviour for the adsorption of n-butyl alcohol and homologous primary alcohols at the air-water interface, and thus we have to deal here with a more general aspect of adsorption of primary alcohols at interfaces.

From the θ–c_a relation at $c_a > c_a{}^l$ the GIBBS free energy of adsorption, ΔG, can be again calculated with the help of equation (5–5). ΔG thus found is also tabulated in table 5–4 for all the alcohols. These values can be seen to match rather well with those of table 5–3. We will consider them again in section 5.2.3.2.

It is striking that alcohols with a high value of ΔG (i.e. relatively strong adsorption), nevertheless show an S-shape isotherm (table 5–2), whereas the relatively low ΔG values correspond with a LANGMUIR appearance of the isotherm. Although one is tempted to think in terms of rupture of a rigid water layer at low alcohol coverage as the origin of the S-shape, a detailed explanation, taking into account all aspects of the problem, is very difficult to give.

When it is assumed that $\Delta n_w{}^{max}$ is the same for all alcohols, the differences in $\Delta E_{z.p.c.}{}^{max}$ for the individual alcohols can be caused only by a difference in the second term of the right hand side of eq. (5–7). This second term, however, contains three unknown parameters, which cannot be evaluated in an independent way, and a quantitative interpretation of the differences on the basis of this equation would be rather arbitrary. Nevertheless one important conclusion

with respect to the orientation of the adsorbed straight chain alcohols can possibly be drawn from table 5–4.

BOCKRIS, DEVANATHAN and MÜLLER (1963) have shown that on mercury straight chain alcohols are adsorbed with their paraffinic chains perpendicular to the interface and the OH-group in the solution (fig. 5–12–a). Experimental evidence is presented for this conclusion, while it is shown that the given configuration is to be preferred above its alternatives in view of their relative free energies of adsorption. These alternative configurations are: a. adsorption of the molecule perpendicular to the interface but with the OH-group directed towards the mercury (fig. 5–12–b) and b. adsorption of the molecule with the hydrocarbon chain flat on the adsorbing surface (fig. 5–12–c). Their theoretical considerations applying to the AgI system as well as to the Hg system, it is very likely that on AgI straight chain alcohols are also adsorbed with the hydrocarbon chain perpendicular to the interface and the OH-group in the solution. The dipole of the primary alcohols is directed then with its negative pole to the AgI, which is also assumed to be the case with the dipoles of adsorbed water at the zero point of charge. As n_a is equal for all primary alcohols and the values of μ and ε in solution are almost the same for n-propyl- and n-butyl alcohol it can be expected that $\Delta E_{z.p.c.}^{max}$ will be about the same for these two alcohols. The OH-group of adsorbed sec. butyl alcohol, on the contrary, will be almost parallel to the interface (fig. 5–12–d), so that $n_a\mu_a/\varepsilon_a$ is virtually negligible for this compound. It can therefore be expected that $\Delta E_{z.p.c.}^{max}$ is larger for sec.

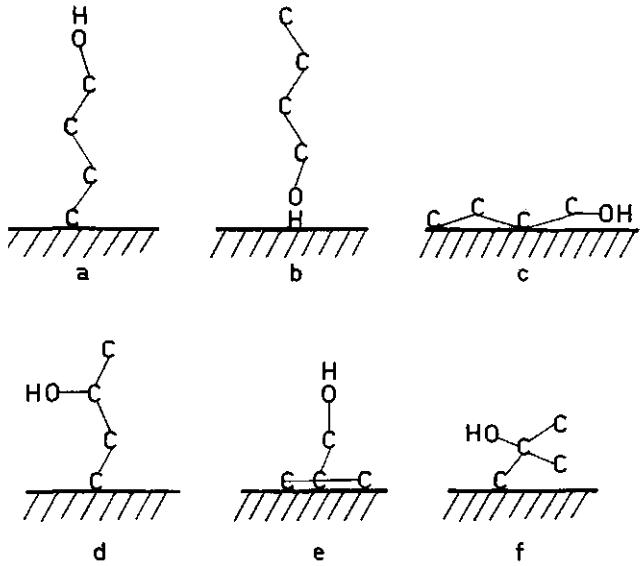

FIGURE 5–12. Schematic representation of the orientation of the alcohols in the adsorbed state. a, b and c: n-butyl alcohol; d: sec. butyl alcohol; e: iso-butyl alcohol; f: tert. butyl alcohol

butyl- than for n-propyl- and n-butyl alcohol. These predictions are confirmed completely by the values of table 5–4, which is a strong support for the postulated configuration.

As to the orientation of iso-butyl- and tert. butyl alcohol in the adsorbed state the following may be noted. If iso-butyl alcohol is adsorbed with the three OH-free C atoms flat on the AgI, the OH-group is almost perpendicular to the interface (fig. 5–12–e). This results in a larger value of μ_a/ε_a than in the case of the primary alcohols because there the OH-group makes an angle with the interface, while the bulk ε is almost the same in both cases. The number of adsorbed iso-butyl alcohol molecules per cm^2 is less, however, than in the case of the primary alcohols, counteracting the increased μ_a. In fact $\Delta E_{z.p.c.}{}^{max}$ is smaller for iso-butyl- than for n-butyl alcohol, so that the increased value of μ_a/ε_a predominates. All orientations of the compound other than the one postulated here would bring about a smaller value of μ_a/ε_a and are improbable therefore. For tert. butyl alcohol $\Delta E_{z.p.c.}{}^{max}$ amounts to a high value; this would imply that the molecule is adsorbed in such a way as to give a small value of μ_a/ε_a, which means a position in which the OH-group is rather parallel to the interface (fig. 5–12–f). As compared to the postulated orientation of iso-butyl alcohol, this orientation does not seem to be very probable however, and we believe therefore that the analysis breaks down here.

5.2.3.2 Adsorption of alcohols at the charge of maximum adsorption

The adsorption of neutral compounds on a charged surface is maximal at that surface charge where the change in GIBBS free energy of the electrical double layer upon adsorption is maximal. FRUMKIN (1926) derived an equation relating this change in GIBBS free energy to the surface charge and some other parameters of the double layer. From the FRUMKIN-equation PARSONS (1963) derived that the surface charge at the adsorption maximum, σ_m, is given by the relation

$$\sigma_m = -\frac{4\pi\,(\mu/\varepsilon - \mu'/\varepsilon')}{(1/K' - 1/K)S} \qquad (5\text{–}11)$$

K = integral capacity per cm^2 of the base solution in the absence of adsorbate
ε = dielectric constant in the double layer in the absence of adsorbate
μ = component perpendicular to the interface of the dipole moment of an area S of the double layer in the absence of adsorbate
S = area occupied by one adsorbed molecule
K', μ' and ε' have the same meaning as K, μ, and ε except that they apply to the surface covered completely with adsorbate. All these symbols are defined at the adsorption maximum.

Let the number of adsorbed molecules per cm^2 at complete coverage of the surface be given by N_a, so that $N_aS = 1$. Then

$$\theta = n_a/N_a = n_aS/N_aS = n_aS \qquad (5\text{–}12)$$

Hence, multiplication of both sides of eq. (5–11) by n_a and some rearrangement results in

$$(\sigma_m/K' - \sigma_m/K)\theta = -4\pi n_a(\mu/\varepsilon - \mu'/\varepsilon') \qquad (5\text{–}13)$$

We may set $\sigma_m/K = \psi_{m,\theta=0}$ and $\sigma_m/K' = \psi_{m,\theta=1}$, where $\psi_{m,\theta=0}$ and $\psi_{m,\theta=1}$ are the potential differences across the double layer at the adsorption maximum in the absence of and at complete coverage with adsorbate respectively. As the maximum is located at a constant cell-EMF the difference between $\psi_{m,\theta=0}$ and $\psi_{m,\theta=1}$ is caused only by the change in $E_{z.p.c.}$ accompanying adsorption, so that

$$(\psi_{m,\theta=1} - \psi_{m,\theta=0}) = \Delta E_{z.p.c.}^{max}$$

Assigning a reasonable value to the area of an adsorbed alcohol molecule, (e.g. 25 Å^2), one can conclude from the desorption curves that θ is almost independent of E between adsorption maximum and zero point of charge (left hand side of fig. 5–9). According to eq. (5–9) we may say

$$\Delta E_{z.p.c.}^{max}\,\theta = (\psi_{m,\theta} - \psi_{m,\theta=0})$$

where $\psi_{m,\theta}$ represents the potential difference across the double layer at an intermediate value of θ; $\psi_{m,\theta}$ is equal to σ_m/K_θ, with K_θ = integral capacity per cm^2 at the adsorption maximum at a degree of coverage θ.

Altogether eq. (5–13) changes into

$$\sigma_m/K_\theta - \sigma_m/K = \sigma_m(K - K_\theta)/KK_\theta = -4\pi n_a(\mu/\varepsilon - \mu'/\varepsilon') \qquad (5\text{–}14)$$

from which can be derived

$$n_a = -\frac{\psi_{m,\theta}(K - K_\theta)}{4\pi(\mu/\varepsilon - \mu'/\varepsilon')K} \qquad (5\text{–}15)$$

Taking all constant factors together, eq. (5–15) can also be written

$$n_a = \text{constant.}\ \psi_{m,\theta}(K - K_\theta)/K \qquad (5\text{–}16)$$

When it is realized that $\psi_{m,\theta}$ and K_θ are the values of ψ_m and K at the concentration c_a causing the degree of surface coverage θ, n_a can be evaluated as a function of c_a, except for a constant factor, from experimental values of ψ_{m,c_a}, K and K_{c_a}. A drawback of this method is that the integral capacities K and K_{c_a} at the adsorption maximum cannot always be determined, because the σ–E curves do not extend sufficiently far to reach the zero point of charge for all

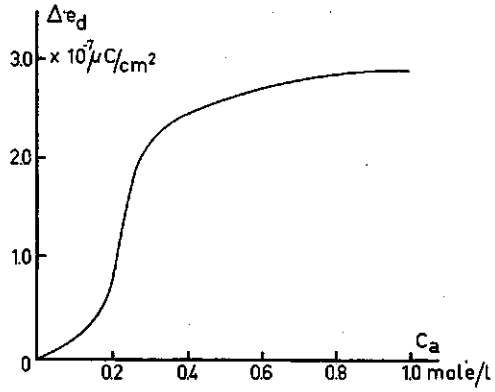

FIGURE 5–13.
Change in dipolar charge/cm², Δe_d, at the adsorption maximum as a function of alcohol concentration, c_a, for n-butyl alcohol

concentrations. Instead of K and K_{ca} we use therefore the differential capacities C and C_{ca}. These are not necessarily equal to the integral capacities. However, the ratio between $(C - C_{ca})/C$ and $(K - K_{ca})/K$ is estimated to be roughly independent of c_a; this justifies the applied procedure.

C being independent of c_a it can be taken up in the constant of eq. (5–16), and as the product $\psi_{m,ca}(C - C_{ca})$ virtually represents a change in dipole charge, Δe_d, the result of the present analysis for n-butyl alcohol is given in fig. 5–13 as a Δe_d versus c_a curve[1].

In the same way as was done for $\Delta E_{z.p.c.}$ it was investigated whether there is a concentration range in which a LANGMUIR isotherm fits the results despite an S-shape appearance of the complete figure. In fact, this appeared to be the case again for most alcohols. Values of θ necessary for the calculation of ΔG on the basis of eq. (5–5) were obtained then as $\theta_m = \Delta e_d/\Delta e_d^{max}$, and are given in

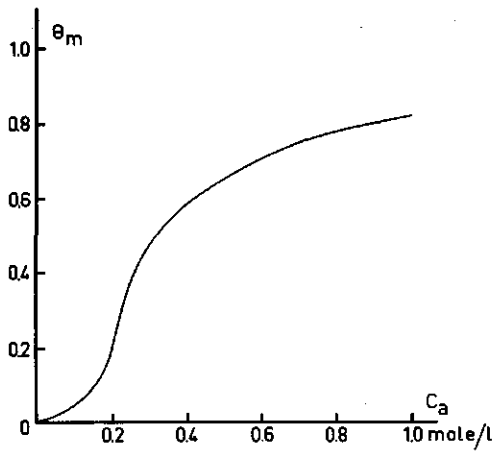

FIGURE 5–14.
Degree of surface coverage at the adsorption maximum, θ_m, as a function of alcohol concentration, c_a, for n-butyl alcohol

[1] A similar analysis, starting with an equation for the potential drop in the double layer instead of the charge, has been given before (BIJSTERBOSCH and LYKLEMA, 1964), but the charge being a better defined quantity (chapter 4) the present approach is to be preferred in principle. However, the result of both analyses is the same.

TABLE 5–5. Characteristics of the adsorption at the adsorption maximum. Explanation in the text

Alcohol	c_a^l mole/l	Δe_d^{max} esu/cm^2	$-\Delta G$ kcal/mole
n-propyl	1.5	2630	2.2
n-butyl	0.5	1560	3.1
iso-butyl	0.7	2410	3.1
sec.butyl	0.8	4000	2.5
tert.butyl	—	—	—

fig. 5–14 as a function of c_a for n-butyl alcohol. The characteristics found by these analyses are compiled in table 5–5. In this table Δe_d^{max} is the maximum obtainable value of Δe_d; c_a^l and ΔG have the same meaning as in table 5–4.

In fig. 5–15, the figures 5–11 and 5–14 are combined. That the two lines in this figure are close together could be expected, because desorption is small between the zero point of charge and the adsorption maximum, and also because the $\theta_{z.p.c.}$ values of fig. 5–11 have been used to a certain extent in the analysis of this section. Agreement is very good at high values of c_a, which is also reflected in the close agreement between the ΔG values for n-butyl alcohol in tables 5–4 and 5–5. Altogether fig. 5–15 is an indication of the overall accuracy of the assumptions made and the experimental values used in both methods of approach.

For the other alcohols the counterparts of fig. 5–15 show about the same agreement between both methods. In fact the agreement is somewhat less for n-propyl- and sec. butyl alcohol (in both cases $\theta_{z.p.c.}$ is always higher than θ_m) but better for iso-butyl alcohol. The higher the concentration the better the agreement, however, which is reflected again in the ΔG values of tables 5–4 and 5–5.

Three remarks have yet to be made about table 5–5. They deal with the values of Δe_d^{max}, with the water orientation at the adsorption maximum, and with the ΔG-values.

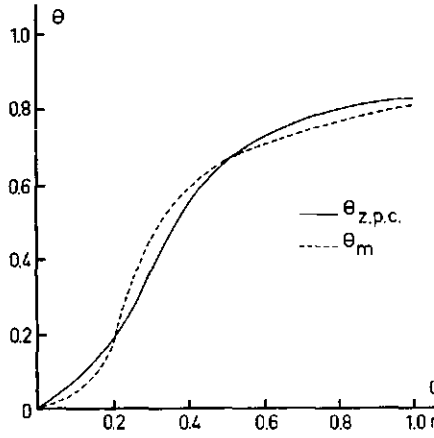

FIGURE 5–15.
Degree of surface coverage at the zero point of charge, $\theta_{z.p.c.}$, and degree of surface coverage at the adsorption maximum, θ_m, as a function of alcohol concentration, c_a, for n-butyl alcohol

The quantity Δe_d^{max} consists of two contributions, one of which is due to the disappearance of water from the surface upon alcohol adsorption and the other is due to the adsorbed alcohol itself. The last contribution will be minimal for that alcohol which contributes the smallest value of the perpendicular component of the dipole moment. In the preceding section it has been shown that this will occur for sec. butyl alcohol, and from table 5–5 it is seen that Δe_d^{max} has indeed the largest value for this alcohol. The values of Δe_d^{max} for the other alcohols are also qualitatively consistent with the model proposed in section 5.2.3.1., except in the case of n-butyl alcohol where Δe_d^{max} is far less than could be expected. No reasonable explanation for this anomaly can be given.

From a physical point of view one could imagine that alcohol adsorption is maximal when water orientation at the interface is minimal. This water orientation could probably increase at surface charges different from σ_m in such a way that the dipoles tend to orient with the positive pole to the AgI surface at $\sigma < \sigma_m$ and with the negative pole at $\sigma > \sigma_m$. The orientation being completely at random at σ_m in this picture, μ_w would have to be zero. Nevertheless a definite value for Δe_d^{max} is found in the case of sec. butyl alcohol, which is rather surprising. This effect can reasonably be explained however, by assuming the existence of induced dipole moments in the water on the AgI surface, as has been done for water on mercury by MACDONALD and BARLOW (1962), and for several non-polar liquids on a variety of metals by BEWIG and ZISMAN (1964). It can then be concluded that the water structure on the surface is minimal at a negative value of the surface charge, so that at the zero point of charge the H_2O dipoles are directed slightly with the negative pole of their dipoles towards the charge-carrier. This picture is consistent with the remarks made in section 5.2.3.1. with respect to this point, and with the models of MACKOR (1951) and LIJKLEMA (1957).

In the course of our analyses we have found the GIBBS free energy of adsorption ΔG by three more or less independent methods. On comparison of these ΔG values, given in the tables 5–3, 4 and 5, it appears that those of the last two agree very well, as has been mentioned before, and that those of the first deviate slightly. Taking into account the rather arbitrary supposition made in deriving the table 3 values, mutual agreement is reasonable.

One of the factors determining ΔG is the interaction between alcohol and solvent in solution, and with respect to this it is interesting to note the correlation between ΔG and the solubility of the various alcohols in water, as given in table 5–6. Here the ΔG values are those of table 5–4, and ∞ means complete miscibility.

Adsorption of primary straight chain alcohols at several interfaces is known to increase with increasing chain length, when this adsorption is measured at constant alcohol concentration in solution (HANSEN and CRAIG, 1954; KIPLING, 1963). Table 5–6 now shows that this behaviour is also displayed by n-propyl- and n-butyl alcohol at the AgI-water interface. The maximum solubility of primary alcohols in water decreases with increasing chain length, so that like-

TABLE 5–6. Comparison between GIBBS free energy of adsorption, ΔG, and maximum solubility in water for the five alcohols

Alcohol	$-\Delta G$ kcal/mole	Maximum solubility in mole alcohol/liter water
n-propyl	2.2	∞
tert.butyl	2.3	∞
sec.butyl	2.6	1.30
iso-butyl	3.2	1.35
n-butyl	3.2	1.08

wise it can be said that their adsorption increases with decreasing solubility. Table 5–6 suggests that this rule can possibly be extended to other alcohols.

5.2.3.3. Adsorption of alcohols at arbitrary values of the surface charge

The methods of calculation given in the preceding sections are related to rather special constant values of the surface charge, and although important conclusions could be drawn from them, it would be attractive to have a method which provides θ as a function of c_a over a wider range of σ.

FRUMKIN (1926), HANSEN, MINTURN and HICKSON (1956) and DAMASKIN (1964) consider the value of σ on mercury at any concentration c_a to be made up of a linear combination of the σ value in the absence of alcohol and the σ value at complete coverage of the electrode with alcohol. As they consider σ at constant values of the cell-EMF, their basic equation reads

$$\sigma_{E,c_a} = \sigma_E (1 - \theta) + \sigma_{E,\theta=1}\,\theta \qquad (5\text{–}17)$$

σ_{E,c_a} = surface charge per cm^2 at cell-EMF E and concentration c_a of alcohol in solution

σ_E = idem, but in the absence of alcohol

$\sigma_{E,\theta=1}$ = idem, but at complete coverage of the surface with adsorbate

In the common intersection point of our $\sigma - E$ curves $\sigma_E = \sigma_{E,c_a} = \sigma_{E,\theta=1}$, and consequently eq. (5–17) cannot be used for the calculation of θ at this point. In addition to this practical disadvantage, objection can be raised against the constant cell-EMF in eq. (5–17), which does not account for the shift in $E_{z.p.c.}$ upon alcohol addition, so that the physical picture is not very clear. Hence, we propose a modification of eq. (5–17) that maintains the linearity in the charge, but considers the charge at constant values of the potential drop across the inner region of the double layer instead of at constant E. The proposed model gives

$$\sigma_{E'} = \sigma_E (1 - \theta) + \sigma_{E''}\,\theta \qquad (5\text{–}18)$$

$\sigma_{E'}$ = surface charge per cm^2 at cell-EMF E' and alcohol concentration c_a

$\sigma_{E''}$ = surface charge per cm^2 at cell-EMF E'' at complete coverage of the surface with adsorbate

$E' = E + \Delta E_{z.p.c.}{}^{c_a}$

$E'' = E + \Delta E_{z.p.c.}{}^{max}$

$\Delta E_{z.p.c.}{}^{c_a}$ = change in potential of the zero point of charge as measured at concentration c_a.

The definition of $\sigma_{E''}$ implies that at all values of E'' complete coverage of the surface occurs, and this is a simplification because this can only be true at $E'' = E_m$. However, desorption is so small in the available E range that no serious deviations are introduced by applying eq. (5–18) to the experimental $\sigma - E$ graphs. The only difficulty is, that we do not know independently whether at the highest concentration available the surface is covered completely with adsorbate. Thus, only relative values of θ can be calculated. In the present calculation it is assumed arbitrarily that $\theta = 1$ for n-butyl alcohol at $c_a = 1.0$ mole/l. On the basis of this assumption and according to eq. (5–18), the $\theta - c_a$ relation was calculated for several values of the potential drop across the inner region of the double layer. This relation appeared to be independent of the magnitude of this potential drop, thus lending support to the proposed model. From the $\theta - c_a$ relations at constant values of the potential drop, the $\theta - c_a$ relations at constant values of the surface charge were evaluated. As could be expected on the basis of the potential independency, θ vs. c_a appeared to be almost independent of the value of the charge chosen, as can be seen from fig. 5–16. This result is consistent again with the thermodynamically found small desorption values.

Finally in fig. 5–17 the results of the three calculation methods for θ are compared, for which the θ values of fig. 5–16 are fitted to make $\theta = 0.82$ at $c_a = 1.0$ mole/l. Fig. 5–17 for n-butyl alcohol is again representative of all other alcohols. The three lines, calculated according to three different methods for three different values of the surface charge are very close together. As has been pointed out several times before this could be expected in view of the thermodynamic analysis given in section 5.2.1., which showed that the desorption around the adsorption maximum is small. Fig. 5–17 is thus an illustration

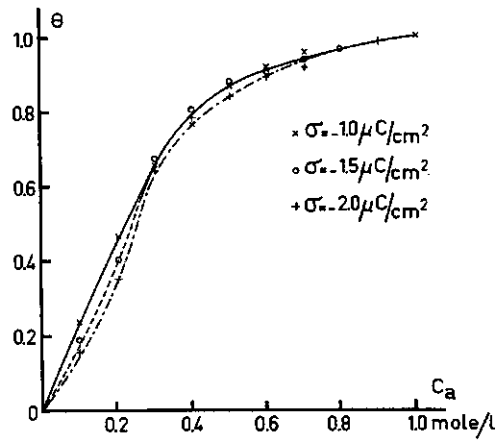

FIGURE 5–16.
Degree of surface coverage, θ, for three different values of the surface charge, as a function of alcohol concentration, c_a, for n-butyl alcohol

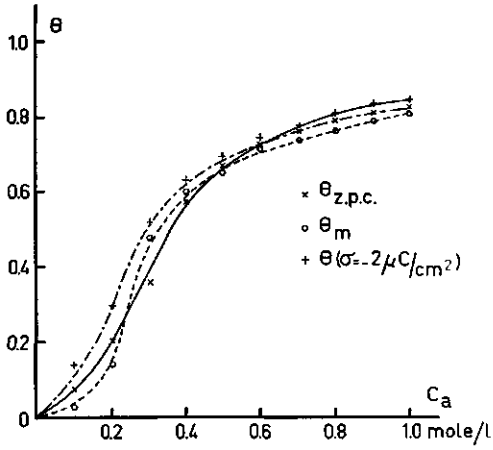

FIGURE 5–17.
Degree of surface coverage as a function of alcohol concentration, c_a, for n-butyl alcohol, calculated according to three different models

of the applicability of the proposed models and the accuracy of the experiments, and it can be concluded that the model presented in eq. (5–18) is also very acceptable. Although it has the disadvantage that it provides only relative values of θ, it is attractive because it is not restricted to one special value of the surface charge, but can cover a wide range of charges.

SUMMARY

The investigations to be described were performed in order to get an insight into the character of the electrical double layer at the silver iodide-electrolyte solution interface in the presence of neutral organic compounds.

In chapter 1 the importance of the study of electrical double layers at interfaces is outlined. Next, attention is paid to the two systems that are most frequently used for the study of double layers, viz. the mercury-solution and the AgI-solution interface. Of these, the Hg system has been investigated most extensively. MACKOR (1951) and LIJKLEMA (1957) have shown that the properties of the AgI system compare well to those on mercury. At present, in the Hg system, much attention is being paid to the influence of organic molecules, and in order to test the cited analogy further, it was considered useful to analyze the double layer in the AgI system in the presence of organic material. As adsorption of organic molecules will affect the water structure at the interface, the system is likewise attractive in principle to test the theory of LYKLEMA and OVERBEEK (1961a) on the mechanics of the slipping process in electrokinetics.

The principle and the practical performance of the potentiometric titration giving the relation between AgI charge, σ, and cell-EMF, E, are described in chapter 2. This technique is fundamentally the same as that used by LIJKLEMA (1957) and his predecessors. However, a number of improvements was introduced leading to a higher accuracy and reproducibility of the results.

In connection with a paper of MIRNIK and DESPOTOVIC (1960), concerning the validity of the NERNST-equation in the case of AgI electrodes, it was investigated rather extensively whether the AgI electrodes used in the present investigations satisfy this equation. In contradistinction to the cited authors, it is concluded that this is indeed the case even at low concentrations of potential determining ions.

The zero point of charge of the precipitates as a function of the concentration of organic compound was determined by streaming potential measurements. This technique is described at the end of chapter 2.

According to the theory of LYKLEMA and OVERBEEK (1961a) the mechanism of the slipping process in electrokinetics is determined by geometrical factors and the influence of the field strength on the viscosity in the double layer (chapter 3). For a quantitative test of this theory one needs a system in which these factors are both operative. As the AgI-solution interface probably meets this requirement, it is investigated whether electrokinetic measurements in this system can yield reliable values of the ζ-potential. It appears that this is not the case, neither with electrophoresis nor with streaming potential measurements. The electrophoretic mobility of negatively charged AgI particles as a function of pAg appears to be constant over a large range. This is also the case in the presence of several concentrations of n-butyl alcohol. The value of this constant mobility decreases approximately linearly with the increase in viscosity of the solvent caused by the addition of alcohol.

The amount of potential determining ions adsorbed at the interface can only be converted into a specific surface charge if the specific surface area of the AgI is known. Some methods for determination of this surface area are described in chapter 4. It appears that the value of this quantity is independent of the amount of AgI present in a given volume of solution; for different samples it amounts to 1 to 3 m^2/gram. The charge is shown to be distributed uniformly over the surface. However, it appears that the AgI charge is not a pure surface charge, but that it extends as a space charge inside the solid material. Consequently a part of the potential difference between AgI and solution, the magnitude of which depends on the charge, is situated in the AgI itself. This effect, as well as the possibility of a change in χ-potential at the interface, has to be accounted for when splitting up experimental changes in cell-EMF into separate potentials. However, the magnitude of the part of the potential residing in the solid phase cannot be calculated exactly as yet.

In an appendix to chapter 4 it is shown that the field strength and the charge distribution in the liquid part of the double layer are independent of the character of the AgI charge.

In chapter 5, $\sigma - E$ relations for urea and a number of alcohols are given as a function of their concentration in, usually, 10^{-1} N KNO_3 solutions. The shifts of the zero points of charge as a function of the alcohol concentration in 10^{-3} N KNO_3 solution, as determined by the streaming potential technique, are also given. The $\sigma - E$ curves for n-butyl alcohol show a close resemblance to those on mercury, as determined by BLOMGREN, BOCKRIS and JESCH (1961). Initially relatively high negative charges become more positive as a result of alcohol addition, whereas low negative and positive charges become more negative. At a given value E_m of the cell-EMF all $\sigma - E$ curves have one common intersection point. Thermodynamic analysis shows that at this common intersection point the alcohol adsorption is maximal, while this adsorption decreases the more the cell-EMF differs from E_m, either in a positive or negative direction. The E range is too small, however, to arrive at complete desorption, so that absolute surface excesses cannot be determined in this way. In the accessible E range the desorption curves show a close analogy with those on mercury. In the AgI case, however, a higher alcohol concentration is required to get the same desorption as on Hg. This qualitative analogy was used to calculate the GIBBS free energy of adsorption of alcohols on AgI (ΔG_{AgI}) from ΔG_{Hg} on the basis of a LANGMUIR type isotherm. ΔG_{AgI} appears to be less negative than ΔG_{Hg}.

In the presence of urea, the $\sigma - E$ curves are practically indistinguishable at high negative charge, but when E becomes more positive the charge also becomes more positive upon urea addition. This is just the reverse effect to that with the alcohols. The thermodynamic analysis consequently shows that urea adsorption is minimal at high negative E, and increases as E becomes more positive. Probably this can be ascribed to chemisorption.

As the thermodynamic analysis cannot yield absolute adsorption values the alcohol adsorption is derived from the experimental results in the form of the degree of surface coverage θ with the help of three model considerations. In the

elaboration of these models usually n-butyl alcohol is chosen as the example.

The first model states that at the zero point of charge the adsorption is proportional to the measured shift of this point. As this shift obeys a LANGMUIR isotherm at higher concentrations, the saturation value of the shift can be found, and the experimental shifts can be converted into θ values.

The second model refers to the charge at the adsorption maximum, and is based on a theory of FRUMKIN (1926) and PARSONS (1963), relating this charge to a number of double layer parameters. Application of this theory, again in combination with the LANGMUIR isotherm, enables one to calculate θ once more as a function of the alcohol concentration c_a in solution. The $\theta - c_a$ relations thus found resemble closely those of the first model, which could be expected on account of the thermodynamically found small desorption in the range between both corresponding charges. From the $\theta - c_a$ relations found by these two models, ΔG_{AgI} is derived again on the basis of the LANGMUIR isotherm mentioned already. The resulting mutual agreement is very good, while the values fit satisfactorily to those derived from the desorption curves. ΔG_{AgI} appears to be more negative, the less the alcohol involved is soluble in water. This agrees with the findings for adsorption of primary straight chain alcohols at other interfaces.

As to the orientation of the alcohols in the adsorbed state, it is concluded that the straight chain alcohols are oriented with their paraffinic chain perpendicular to the AgI surface and with the OH-group in the solution. In this respect AgI and Hg again behave identically. For the branched alcohols, the OH-group is probably also as far from the AgI surface as possible.

The third model, being a variation on a model used on Hg by several authors, states that at constant potential difference across the inner part of the double layer, the charge at any arbitrary value of c_a is given by a linear combination of the charge in the absence of alcohol and the charge at complete coverage of the surface with adsorbate. The advantage of this picture is that it is not restricted to one special value of the charge. However, the disadvantage is that the concentration at which the surface is covered completely must be known in advance. When in the present model a $\theta - c_a$ combination is substituted as found with one of the preceding models, the $\theta - c_a$ relation appears to be practically equal to that of the two other models.

Since in the three different models different experimental data are used, the good mutual agreement is a strong indication that the presented adsorption picture is correct.

ACKNOWLEDGEMENTS

This work was performed partly in the van 't Hoff laboratory of the State University of Utrecht and partly in the laboratory for physical and colloid chemistry of the Agricultural University of Wageningen.

The author is very grateful to Prof. Dr. J. TH. G. OVERBEEK and Prof. Dr. J. LYKLEMA for their interest, stimulating discussions and guidance during the whole course of this work.

The friendliness and helpfulness of all those active in both laboratories has been of great profit and is gratefully acknowledged.

SAMENVATTING

Het doel van de verrichte onderzoekingen was, een inzicht te krijgen in het karakter van de electrische dubbellaag aan het grensvlak zilverjodide-electrolytoplossing in aanwezigheid van neutrale organische verbindingen.

In hoofdstuk 1 wordt eerst de betekenis geschetst van het onderzoek van de electrische dubbellaag aan fasegrenzen in het algemeen. Vervolgens wordt nader ingegaan op de twee systemen die voor bestudering van deze dubbellaag het meest gebruikt zijn, n.l. het kwik-oplossing-, en het AgJ-oplossing grensvlak. Van deze twee is het Hg-systeem het intensiefst onderzocht, maar o.a. door MACKOR (1951) en LIJKLEMA (1957) is aangetoond dat de resultaten in het AgJ-systeem grote gelijkenis vertonen met die op kwik. In het Hg-systeem wordt op het ogenblik veel aandacht besteed aan de invloed van organische moleculen, en om de eerder genoemde analogie nader te toetsen werd het nuttig geoordeeld ook de dubbellaag in het AgJ-systeem in aanwezigheid van organisch materiaal te analyseren. Aangezien adsorptie van organische moleculen invloed zal hebben op de waterstructuur in het grensvlak, is het systeem in principe tevens aantrekkelijk om de theorie van LYKLEMA en OVERBEEK (1961 a) betreffende het afschuifmechanisme in de electrokinetiek te toetsen.

Het principe en de practische uitvoering van de potentiometrische titratie die het verband levert tussen AgJ-lading, σ, en cel-EMK, E, worden beschreven in hoofdstuk 2. Deze techniek is in wezen dezelfde als die welke gebruikt werd door LIJKLEMA (1957) en zijn voorgangers. Er werden echter enige verbeteringen aangebracht die tot een grotere nauwkeurigheid en reproduceerbaarheid van de uitkomsten leidden. Naar aanleiding van een artikel van MIRNIK en DESPOTOVIC (1960) over de geldigheid van de NERNST-vergelijking in het geval van AgJ-electrodes werd vrij uitvoerig onderzocht of de gebruikte AgJ-electrodes aan de vergelijking van NERNST voldoen. In tegenstelling tot genoemde auteurs wordt geconcludeerd dat dit, ook bij lage concentraties potentiaal-bepalende ionen, inderdaad het geval is.

Het ladingsnulpunt van de gebruikte neerslagen als functie van de concentratie organische component werd bepaald met behulp van stromingspotentiaal metingen, die aan het eind van hoofdstuk 2 beschreven worden.

Volgens de theorie van LYKLEMA en OVERBEEK (1961 a) wordt het afschuifmechanisme in de electrokinetiek bepaald door geometrische omstandigheden en de invloed van de veldsterkte op de viscositeit in de dubbellaag (hoofdstuk 3). Voor een kwantitatieve toetsing van deze theorie moet men beschikken over een systeem waarin deze beide factoren werkzaam zijn. Aangezien het AgJ-oplossing grensvlak waarschijnlijk aan deze eis voldoet, wordt nagegaan of electrokinetische metingen aan dit systeem betrouwbare waarden van de ζ-potentiaal kunnen leveren. Het blijkt dat dit nóch met electroforese- nóch met stromingspotentiaal metingen het geval is. De electroforesesnelheid van negatief geladen AgJ-deeltjes als functie van de pAg blijkt over een groot traject constant te zijn. Dit is eveneens het geval in aanwezigheid van verschillende concentraties

n-butylalcohol. De waarde van deze constante snelheid daalt ongeveer lineair met de viscositeitstoename van het oplosmiddel ten gevolge van de alcoholtoevoeging.

De hoeveelheid potentiaal-bepalende ionen die aan het grensvlak geadsorbeerd is, kan alleen omgerekend worden in een specifieke oppervlaktelading als het specifieke oppervlak van het AgJ bekend is. Enige methodes om dit oppervlak te bepalen worden behandeld in hoofdstuk 4. Het blijkt dat de grootte van het specifieke oppervlak onafhankelijk is van de hoeveelheid AgJ die zich in een bepaald vloeistofvolume bevindt, en dat de waarde voor verschillende monsters 1 tot 3 m^2/gram bedraagt. De vraag of de lading gelijkmatig over het oppervlak verdeeld is, wordt bevestigend beantwoord. Het blijkt echter dat de AgJ-lading geen zuivere wandlading is, maar zich als een ruimtelading in het binnenste van de vaste stof uitstrekt. Ten gevolge hiervan zit een, met de lading veranderend, deel van het potentiaalverschil tussen AgJ en oplossing in het AgJ zelf. Daarmee, evenals met een mogelijke verandering van de χ-potentiaal aan het grensvlak, dient rekening gehouden te worden bij het opsplitsen van gemeten veranderingen in de cel-EMK in afzonderlijke potentialen. De grootte van het potentiaalverschil in de vaste fase laat zich vooralsnog echter niet exact berekenen.

In een appendix aan hoofdstuk 4 wordt aangetoond dat de veldsterkte en de ladingsverdeling in het vloeistofgedeelte van de dubbellaag onafhankelijk zijn van het karakter van de AgJ-lading.

In hoofdstuk 5 worden de $\sigma - E$ relaties gegeven voor ureum en een aantal alcoholen, als functie van hun concentratie in, voornamelijk, 10^{-1} N KNO_3 oplossingen. De verschuivingen van het ladingsnulpunt als functie van de alcoholconcentratie in 10^{-3} N KNO_3 oplossing zoals bepaald met behulp van de stromingspotentiaal techniek, worden eveneens gegeven. De $\sigma - E$ curven voor n-butylalcohol vertonen sterke gelijkenis met die welke door BLOMGREN, BOCKRIS en JESCH (1961) op Hg bepaald werden: aanvankelijk relatief hoge negatieve ladingen worden positiever ten gevolge van alcoholtoevoeging, terwijl lage negatieve en positieve ladingen juist negatiever worden. Bij één bepaalde waarde E_m van de cel-EMK gaan alle $\sigma - E$ curven door één gezamenlijk snijpunt. Thermodynamische analyse toont aan dat in dit gezamenlijk snijpunt de adsorptie van alcohol maximaal is en dat deze afneemt naarmate de cel-EMK verder van E_m verwijderd is, hetzij in positieve, hetzij in negatieve richting. Het E-traject is echter te kort om tot volledige desorptie te geraken, zodat absolute oppervlakte-overschotten op deze manier niet bepaald kunnen worden. De gevonden desorptiecurven vertonen in het bereikbare gebied grote analogie met die op Hg; bij AgJ is echter een hogere alcoholconcentratie nodig om een zelfde resultaat te verkrijgen als bij Hg. Van deze kwalitatieve analogie werd gebruik gemaakt om op basis van een LANGMUIR-type isotherm de vrije adsorptie-enthalpie voor adsorptie van alcoholen op AgJ (ΔG_{AgJ}) te berekenen uit ΔG_{Hg}. ΔG_{AgJ} blijkt minder negatief te zijn dan ΔG_{Hg}.

In aanwezigheid van ureum zijn de $\sigma - E$ curven bij hoge negatieve lading practisch ononderscheidbaar, maar naarmate de E positiever wordt, wordt de

lading ten gevolge van ureum toevoeging ook steeds positiever, dus juist het omgekeerde effect als bij de alcoholen. De thermodynamische analyse toont dan ook aan dat de ureumadsorptie minimaal is bij hoge negatieve E en toeneemt naarmate de E positiever wordt. Waarschijnlijk is dit toe te schrijven aan het optreden van chemisorptie.

Aangezien de thermodynamische analyse geen absolute adsorptiewaarden op kan leveren, wordt de alcoholadsorptie, in de vorm van de bedekkingsgraad θ, uit de experimentele resultaten afgeleid met behulp van een drietal modelvoorstellingen. Bij de uitwerking van deze modellen wordt meestal n-butylalcohol als voorbeeld gekozen.

Het eerste model stelt, dat in het ladingsnulpunt de adsorptie evenredig is met de gemeten verschuiving van dit punt. Aangezien deze verschuiving bij hogere concentraties aan een LANGMUIR-isotherm voldoet is de verzadigingswaarde van de verschuiving te vinden, en kunnen de gemeten verschuivingen omgerekend worden in θ-waarden.

Het tweede model heeft betrekking op de lading van het adsorptiemaximum en is gebaseerd op een theorie van FRUMKIN (1926) en PARSONS (1963) die deze lading koppelt aan een aantal dubbellaag parameters. Toepassing van deze theorie, alsmede opnieuw de toepassing van de LANGMUIR-isotherm, stelt ons in staat wederom θ als functie van de alcoholcontratie c_a in oplossing te berekenen. De aldus gevonden $\theta - c_a$ relaties lijken zeer sterk op die van het eerste model, wat ook verwacht mag worden op grond van de thermodynamisch gevonden kleine desorptie in het traject tussen beide corresponderende ladingen. Uit de met beide modellen gevonden $\theta - c_a$ relaties wordt op basis van de reeds genoemde LANGMUIR-isotherm opnieuw ΔG_{AgJ} bepaald. De onderlinge overeenstemming is daarbij zeer goed, terwijl de waarden bevredigend aansluiten bij die welke gevonden werden uit de desorptiekrommen. ΔG_{AgJ} blijkt des te negatiever te zijn naarmate de betrokken alcohol slechter in water oplosbaar is. Dit is in overeenstemming met hetgeen bij adsorptie van primaire rechte keten alcoholen aan andere grensvlakken gevonden is.

Wat de oriëntatie van de alcoholen in geadsorbeerde toestand betreft wordt geconcludeerd dat de rechte keten alcoholen met hun paraffinestaart loodrecht op het AgJ-oppervlak staan, en zich met de polaire OH-groep in de oplossing bevinden. Ook in dit opzicht gedragen AgJ en Hg zich identiek. Bij de vertakte alcoholen bevindt de OH-groep zich waarschijnlijk ook steeds zo ver mogelijk van het AgJ-oppervlak.

Het derde model, dat een variatie is op een model dat door verschillende auteurs op Hg gebruikt wordt, gaat er van uit dat bij constant potentiaalverschil over het binnenste deel van de dubbellaag de lading bij iedere willekeurige waarde van c_a gegeven wordt door een lineaire combinatie van de lading bij afwezigheid van alcohol en de lading bij volledige bedekking van het oppervlak met adsorbaat. Het voordeel van dit beeld is, dat het zich niet beperkt tot één bepaalde waarde van de lading, maar veel algemener is. Het nadeel is daarentegen dat bij voorbaat bekend moet zijn, bij welke concentratie het oppervlak geheel vol zit. Wanneer in het onderhavige model een bepaalde $\theta - c_a$ combi-

natie wordt gesubstitueerd, die gevonden is met een van de beide andere modellen, dan blijkt het $\theta - c_a$ verloop weer practisch gelijk te zijn aan dat van die beide andere modellen.

Aangezien bij de drie verschillende modellen gebruik gemaakt wordt van verschillende experimentele gegevens, is de goede onderlinge overeenstemming een sterke aanwijzing voor de juistheid van het gevormde adsorptiebeeld.

REFERENCES

AGAR, G. A. (1961). Thesis, MIT, Cambridge U.S.A.

AVGUL', N. N., KISELEV, A. V., and LYGINA, I. A. (1961). Kolloidny Zhurn. (English translation) **23**, 429.

BASINSKI, A. (1941). Rec. Trav. Chim. **60**, 267.

BEWIG, K. W., and ZISMAN, W. A. (1964). J. Phys. Chem. **68**, 1804.

BLOMGREN, E., BOCKRIS, J. O. 'M., JESCH, C. (1961). J. Phys. Chem. **65**, 2000.

BOCKRIS, J. O. 'M., DEVANATHAN, M. A. V., and MÜLLER, K. (1963). Proc. Roy. Soc. A **274**, 55.

BROWN, A. S. (1934). J. Am. Chem. Soc. **56**, 646.

DE BRUYN, H. (1942). Rec. Trav. Chim. **61**, 5, 12.

BRYANT, G. W., HALLETT, J., and MASON, B. J. (1959). J. Phys. Chem. Solids **12**, 189.

BUCHANAN, A.S., and HEYMANN, E. (1948). Proc. Roy. Soc. A **195**, 150.

BURLEY, G. (1963). J. Chem. Phys. **38**, 2807.

BIJSTERBOSCH, B. H., and LYKLEMA, J. (1964). Proceedings 4th International Congress on Surface Active Substances, Brussels.

CORRIN, M. L., and STORM, N. S. (1963). J. Phys. Chem. **67**, 1509.

DAMASKIN, B. B. (1964). Electrochim. Acta **9**, 231.

DERJAGUIN, B. V., and LANDAU, L. (1941). Acta Physico Chim. U.R.S.S. **14**, 633.

DEVANATHAN, M. A. V. (1962). Proc. Roy. Soc. A **267**, 256.

DOUGLAS, H. W., and BURDEN, J. (1959). Trans. Faraday Soc. **55**, 350.

EDWARDS, G. R., EVANS, L. F., and LA MER, V. K. (1962). J. Colloid Sci. **17**, 749.

FRUMKIN, A. N. (1926). Z. Physik **35**, 792.

FRUMKIN, A. (1961). Electrochim. Acta **5**, 265.

FYFE, W. S. (1955). J. Chem. Soc., 1032.

VAN GILS, G. E., and KRUYT, H. R. (1936). Kolloid-Beih. **45**, 60.

GRAHAME, D. C., (1947). Chem. Revs. **41**, 441.

GRIMLEY, T. B., and MOTT, N. F. (1947). Discussions Faraday Soc. **1**, 3.

GRIMLEY, T. B. (1950). Proc. Roy. Soc. A **201**, 40.

GUTOFF, E. B., ROTH, P. H., and STEIGMANN, A. E. (1963). J. Phys. Chem. **67**, 2366.

HANSEN, R. S., and CRAIG, R. P. (1954). J. Phys. Chem. **58**, 211.

HANSEN, R. S., MINTURN, R. E., and HICKSON, D. A. (1956). J. Phys. Chem. **60**, 1185.

HANSEN, R. S., KELSH, D. J., and GRANTHAM, D. H. (1963). J. Phys. Chem. **67**, 2316.

HAYDON, D. A., (1964). In Recent Progress in Surface Science, Vol. 1 (Acad. Press, New York, London).

HERZ, A. H., and HELLING, J. O. (1962). J. Colloid Sci. **17**, 293.

VAN DEN HUL, H. J., and LYKLEMA, J. (1964). Proceedings 4th International Congress on Surface Active Substances, Brussels.

HUNTER, R. J., and ALEXANDER, A. E. (1962). J. Colloid Sci. **17**, 781.

IVES, D. J. G., and JANZ, G. J. (1961). Reference Electrodes. (Acad. Press, New York, London) p. 161.

IWASAKI, I., and DE BRUYN, P. L. (1958). J. Phys. Chem. **62**, 594.

JAYCOCK, M. J. (1963). Thesis, Cambridge.

KATZ, U. (1961). Z. Angew. Math. Phys. **12**, 76.

KIPLING, J. J. (1963). J. Colloid Sci. **18**, 502.

KITTEL, H. (1960). Introduction to solid state physics. (Wiley and Sons, Inc., New York).

KLOMPÉ, M. A. M. (1941). Thesis, State University of Utrecht.

KORPI, G. K. (1960). M. Sc. Thesis, MIT, Cambridge, U.S.A.

KRUYT, H. R., and KLOMPÉ, M. A. M. (1942). Kolloid-Beih. **54**, 484.

VAN LAAR, J. A. W. (1952). Thesis, State University of Utrecht.

VAN LAAR, J. A. W. (1955). (To N.V. Philips Gloeilampen Fabrieken, Eindhoven, Netherlands), Dutch Patent 79, 472, Nov. 15.

LEVINE, S., and BELL, G. M. (1963). J. Phys. Chem. **67**, 1408.

LIESER, K. H. (1954). Z. Phys. Chem. (N. F.) **2**, 238.

LIESER, K. H. (1956). Z. Phys. Chem. (N. F.) **9**, 216.
LIJKLEMA, J. (1957). Thesis, State University of Utrecht.
LIJKLEMA, J. (1961). Kolloid-Z. **175**, 129.
LYKLEMA, J., and OVERBEEK, J. TH. G. (1961a). J. Colloid Sci. **16**, 501.
LYKLEMA, J., and OVERBEEK, J. TH. G. (1961b). J. Colloid Sci. **16**, 595.
MACDONALD, J. R., and BARLOW, C. A. (1962). J. Chem. Phys. **36**, 3062.
MACKOR, E. L. (1951). Thesis, State University of Utrecht. Rec. Trav. Chim., **70**, 663, 763.
MIRNIK, M., and DESPOTOVIC, R. (1960). Croat. Chem. Acta, **32**, 139.
VAN OLPHEN, H. (1963). An Introduction to Clay Colloid Chemistry (Interscience Publishers, New York).
OOSTERMAN, J. (1937). Thesis, State University of Utrecht.
OTTEWILL, R. H., and RASTOGI, M. C. (1960). Trans. Faraday Soc. **56**, 880.
OTTEWILL, R. H., and WOODBRIDGE, R. F. (1961). J. Colloid Sci. **16**, 581.
OTTEWILL, R. H., and WOODBRIDGE, R. F. (1964). J. Colloid Sci. **19**, 606.
OVERBEEK, J. TH. G., and WIJGA, P. W. O. (1946). Rec. Trav. Chim. **65**, 556.
OVERBEEK, J. TH. G. (1952). In Colloid Science, H. R. Kruyt ed. (Elsevier, Amsterdam).
OVERBEEK, J. TH. G., and VAN EST, W. T. (1952). Rec. Trav. Chim. **72**, 97. Proc. Kon. Akad. Wetenschap. Amsterdam **A 55**, 347.
PARFITT, G. D., and SMITH, A. L. (1964). Personal communication.
PARKS, G. A., and DE BRUYN, P. L. (1962). J. Phys. Chem. **66**, 967.
PARSONS, R. (1961). Proc. Roy. Soc. **A 261**, 79.
PARSONS, R. (1963). J. Electroanal. Chem. **5**, 397.
RUTGERS, A. J., and NAGELS, P. (1958). J. Colloid Sci. **13**, 140.
SARABY – REINTJES, A. (1963). Thesis, State University of Utrecht.
SCHAPINK, F. W., OUDEMAN, M., LEU, K. W., and HELLE, J. N. (1960). Trans. Faraday Soc. **56**, 415.
SCHENKEL, J. H., and KITCHENER, J. A. (1960). Trans. Faraday Soc. **56**, 161.
SHAPIRO, I., and KOLTHOFF, I. M. (1947). J. Chem. Phys. **15**, 41.
SRIVASTAVA, S. N., and HAYDON, D. A. (1964). Trans. Faraday Soc. **60**, 971.
TELTOW, J. (1950). Ann. Phys. **5**, 63.
TROELSTRA, S. A. (1941). Thesis, State University of Utrecht.
VERWEY, E. J. W., and KRUYT, H. R. (1933). Z. Phys. Chem. **A 167**, 137.
VERWEY, E. J. W., and NIESSEN, K. F. (1939). Phil. Mag. (7) **28**, 435.
VERWEY, E. J. W. and OVERBEEK, J. TH. G. (1948). Theory of the Stability of Lyophobic Colloids (Elsevier, Amsterdam).
WATANABE, A. (1960). Bull. Inst. for Chem. Research, Kyoto University **38**, 179.
WATANABE, A., and GOTOH, R. (1963). Kolloid-Z. **191**, 36.
WIERSEMA, P. H. (1964). Thesis, State University of Utrecht.
WIJGA, P. W. O. (1946). Thesis, State University of Utrecht.

LIST OF SYMBOLS AND ABBREVIATIONS

A small number of symbols has been used for two different quantities. As these different quantities appear in different chapters only, and these chapters are given below, it is assumed that this will not give rise to confusion.

a	activity (chapter 2); a subscript indicates the substance to which the activity applies
a	radius of a spherical colloidal particle (chapter 3)
A	energy required to bring a Ag^+ ion from a lattice site to an interstitial position
$\mathring{A}$	ÅNGSTRØM
b	$\Delta n_w/\Delta n_a$
c	concentration
c_a	alcohol concentration
c_a^l	alcohol concentration above which a LANGMUIR isotherm describes the adsorption
C	differential capacity per cm^2 of the double layer at $E = E_m$ in the absence of adsorbate
C_{c_a}	differential capacity per cm^2 of the double layer at $E = E_m$ for concentration c_a
d	density
D_n	normal component of dielectric displacement
e	elementary charge
e_d	dipole charge
E	cell-EMF
E_c	cell-EMF where $\sigma - E$ curves for urea coincide
E_e	potential of AgI electrode relative to the solution
E_m	cell-EMF at intersection point of $\sigma - E$ curves for alcohols
E_s	potential difference between AgI and solution
$E_{z.p.c.}$	cell-EMF at zero point of charge
$E.M.$	electrophoretic mobility
E'	$E + \Delta E_{z.p.c.}^{c_a}$
E''	$E + \Delta E_{z.p.c.}^{max}$
$E_{0,Ag}, E_{0,I}$	potential of the AgI electrode relative to a standard $AgNO_3$(KI) solution
$E_{0,Ag}'$	$E_{0,Ag} + (RT/F) \ln f_{Ag^+}$

$E_{0,I}'$	$E_{0,I} - (RT/F) \ln f_{I^-}$
$E_{0,Ag}''$, $E_{0,I}''$	cell-EMF at equilibrium between the AgI electrode and a standard $AgNO_3$(KI) solution
f	activity coefficient
F	the FARADAY
IEC	indifferent electrolyte concentration
k	BOLTZMANN constant
K	integral capacity per cm^2 of the double layer at $E = E_m$ in the absence of adsorbate
K_{c_a}	integral capacity per cm^2 of the double layer at $E = E_m$ at concentration c_a
K_θ	integral capacity per cm^2 of the double layer at $E = E_m$ at degree of coverage θ
K'	integral capacity per cm^2 of the double layer at $E = E_m$ at complete coverage of the surface with adsorbate
M	molecular weight
$M\Omega$	mega OHM
n	number of FRENKEL-defects per cm^3
n_a,n_w	number of adsorbed alcohol (water) molecules per cm^2 at arbitrary concentration c_a
n_i	number of charge carriers in phase i
N	number of lattice sites per cm^3
N_a	number of adsorbed alcohol molecules per cm^2 at complete coverage of the surface with adsorbate
$N_{Av.}$	AVOGADRO's number
N'	number of interstitial places per cm^3
pAg, pI	negative logarithm of silver(iodide) concentration
P	hydrostatic pressure
Q	charge enclosed by an arbitrarily chosen closed surface S
R	gas constant
S	arbitrarily chosen closed surface (appendix chapter 4)
S	area occupied by one adsorbed alcohol molecule (chapter 5)
T	absolute temperature
V	streaming potential
V_1,V_2	potentiometer reading
y_i	$e\psi_i/2kT$
z.p.c.	zero point of charge

γ	GIBBS free energy of 1 cm^2 of the interface
Γ_i	surface excess of component i per cm^2
Δ	change in a parameter
Δe_d^{max}	maximum change in e_d obtainable
$\Delta E_{z.p.c.}^{c_a}$	shift in zero point of charge as measured at concentration c_a
$\Delta E_{z.p.c.}^{max}$	maximum change in $E_{z.p.c.}$ obtainable
ΔG	GIBBS free energy of adsorption
Δn_a^{max}	maximum change in n_a obtainable
ε	dielectric constant in the solution (chapter 3)
ε	dielectric constant in the inner part of the double layer at $E = E_m$ in the absence of adsorbate (chapter 5)
$\varepsilon_a, \varepsilon_w$	dielectric constant of the adsorbed alcohol(water) layer
ε_i	dielectric constant in phase i
ε'	dielectric constant in the inner part of the double layer at $E = E_m$ at complete coverage of the surface with adsorbate
ζ	electrokinetic potential
η	viscosity of the solution
θ	degree of surface coverage
$\varkappa$	reciprocal thickness of the diffuse double layer
λ	specific conductivity of the solution
λ_0	specific conductivity of a free 10^{-3} N KNO_3 solution
λ_p	specific conductivity of a AgI plug in equilibrium with a 10^{-3} N KNO_3 solution
μ	component perpendicular to the interface of the dipole moment of an area S of the inner part of the double layer at $E = E_m$ in the absence of adsorbate
μ'	as μ, but at complete coverage of the surface with adsorbate
μ_a, μ_w	component perpendicular to the interface of the dipole moment of adsorbed alcohol(water)molecules
μ_i	chemical potential of component i
σ	surface charge
σ_E	surface charge at cell-EMF E in the absence of alcohol

σ_{E,c_a}	surface charge at cell-EMF E and alcohol concentration c_a
$\sigma_{E,\theta=1}$	surface charge at cell-EMF E at complete coverage of the surface with adsorbate
$\sigma_{E'}$	surface charge at cell-EMF E' and alcohol concentration c_a
$\sigma_{E''}$	surface charge at cell-EMF E'' and complete coverage of the surface with adsorbate
σ_m	surface charge at the intersection point of the $\sigma - E$ curves for the alcohols
χ	potential at the interface, originating from e.g. dipole orientation and polarization
ψ_i	potential drop in phase i
ψ_{m,c_a}	potential difference across the double layer at $E = E_m$ at alcohol concentration c_a
$\psi_{m,\theta=0}$	potential difference across the double layer at $E = E_m$ in the absence of adsorbate
$\psi_{m,\theta}$	potential difference across the double layer at $E = E_m$ at degree of surface coverage θ
$\psi_{m,\theta=1}$	potential difference across the double layer at $E = E_m$ at complete coverage of the surface with adsorbate
ψ_0	surface potential
ψ_δ	potential drop across the diffuse part of the double layer
$(d\psi/dx)_{sol.}$	electrical field strength in solution.